

# An Efficient Subgraph GNN with Provable Substructure Counting Power

Zuoyu Yan  
yanzuoyu3@pku.edu.cn  
Wangxuan Institute of Computer  
Technology, Peking University  
Beijing, China

Junru Zhou  
zml72062@stu.pku.edu.cn  
Institute for Artificial Intelligence,  
Peking University  
Beijing, China

Liangcai Gao\*  
glc@pku.edu.cn  
Wangxuan Institute of Computer  
Technology, Peking University  
Beijing, China

Zhi Tang  
tangzhi@pku.edu.cn  
Wangxuan Institute of Computer  
Technology, Peking University  
Beijing, China

Muhan Zhang\*  
muhan@pku.edu.cn  
Beijing Institute for General Artificial  
Intelligence, Peking University  
Beijing, China

## ABSTRACT

We investigate the enhancement of graph neural networks' (GNNs) representation power through their ability in substructure counting. Recent advances have seen the adoption of subgraph GNNs, which partition an input graph into numerous subgraphs, subsequently applying GNNs to each to augment the graph's overall representation. Despite their ability to identify various substructures, subgraph GNNs are hindered by significant computational and memory costs. In this paper, we tackle a critical question: Is it possible for GNNs to count substructures both **efficiently** and **provably**? Our approach begins with a theoretical demonstration that the distance to rooted nodes in subgraphs is key to boosting the counting power of subgraph GNNs. To avoid the need for repetitively applying GNN across all subgraphs, we introduce precomputed structural embeddings that encapsulate this crucial distance information. Experiments validate that our proposed model retains the counting power of subgraph GNNs while achieving significantly faster performance.

## CCS CONCEPTS

• **Computing methodologies** → **Neural networks; Supervised learning by classification; Supervised learning by regression.**

## KEYWORDS

Subgraph GNN, Count substructures, Subgraph Isomorphism counting, Graph Isomorphism test, Graph Neural Network

### ACM Reference Format:

Zuoyu Yan, Junru Zhou, Liangcai Gao, Zhi Tang, and Muhan Zhang. 2024. An Efficient Subgraph GNN with Provable Substructure Counting Power.

\*Correspondence to Muhan Zhang, and Liangcai Gao

Permission to make digital or hard copies of all or part of this work for personal or classroom use is granted without fee provided that copies are not made or distributed for profit or commercial advantage and that copies bear this notice and the full citation on the first page. Copyrights for components of this work owned by others than the author(s) must be honored. Abstracting with credit is permitted. To copy otherwise, or republish, to post on servers or to redistribute to lists, requires prior specific permission and/or a fee. Request permissions from [permissions@acm.org](mailto:permissions@acm.org).

KDD '24, August 25–29, 2024, Barcelona, Spain

© 2024 Copyright held by the owner/author(s). Publication rights licensed to ACM.

ACM ISBN 979-8-4007-0490-1/24/08

<https://doi.org/10.1145/3637528.3671731>

In *Proceedings of the 30th ACM SIGKDD Conference on Knowledge Discovery and Data Mining (KDD '24)*, August 25–29, 2024, Barcelona, Spain. ACM, Barcelona, BCN, Spain, 20 pages. <https://doi.org/10.1145/3637528.3671731>

## 1 INTRODUCTION

Message Passing Neural Networks (MPNNs) are the most commonly used GNNs. They have achieved remarkable success on graph representation learning [34, 73], and have been widely used in various downstream tasks [70, 88]. However, the representation power of MPNNs is limited [73], thus increasing efforts have been spent on designing more powerful GNNs.

An essential and intuitive way to evaluate the representation power of GNNs is whether they **provably** approximate specific functions, such as counting graph substructures. Substructures often represent meaningful components in graphs and can reveal essential structural insights in chemistry [19, 32], biology [35], and sociology [31]. For instance, in a molecule graph, the presence of a 6-cycle (hexagon) passing through a node suggests its potential association with a benzene ring. Moreover, substructures are closely connected to many fundamental graph properties [57, 63]. In graph representation learning tasks, many targets are unknown or intractable functions of the graph structure which we need to learn from the data. However, MPNNs' substructure counting ability is shown to be very limited, failing to count even triangles [16]. If the underlying graph functions depend on some substructures that the GNN theoretically cannot detect/count, we can never trust its performance on these tasks.

In this paper, we focus on the counting power of GNNs, i.e., whether GNNs can provably count the number of given connected substructures within a graph. Notice that we are not designing models to only count substructures (which can be perfectly done by traditional algorithms), but to propose GNNs with high enough representation power to solve unknown structure-related tasks that we need to learn from the data. In classic works [25], to reach a high representation power, globally expressive models such as 3-WL [45, 64] are needed. However, their high computational costs restrict their universal use in real-world applications.

Recently, a series of works called subgraph GNNs [9, 24, 30, 81, 85, 87] are shown to provably count certain substructures. For an input graph, they first decompose the input graph into a collection

of subgraphs (overlap is allowed) based on certain subgraph selection policies. Then some base GNNs are applied to the extracted subgraphs whose representations are used to enhance the graph representation. Although faster than globally expressive GNNs, they still need to run GNNs over all subgraphs. Therefore they are much slower compared with classic MPNNs, and suffer from high computational cost when encoding large and dense graphs.

Based on the above observation, we raise a nontrivial question: can we count substructures **efficiently and provably** with GNNs, ideally using a similar cost to MPNNs? To answer the above, we decompose it into two sub-questions: (1) what provides the extra representation power of subgraph GNNs compared with classic MPNNs? (2) can we utilize such information efficiently without running GNNs on subgraphs? To answer the first question, we show that the key to boosting the counting power of subgraph GNNs is the **distance** to the rooted nodes within the subgraph. To answer the second question, we find that such distance information can be encoded into a precomputed structural embedding. Combining it with a base GNN, there is no need to run GNNs repeatedly on each subgraph. In this way, we only need to run GNNs on the original graph (augmented with precomputed structural embeddings), while being able to efficiently count substructures.

In summary, our contributions are listed as follows:

(1) We theoretically characterize the general substructure counting power of subgraph GNNs, showing that they are *much more efficient yet nearly as powerful* as globally expressive models.

(2) To accelerate subgraph GNNs, we theoretically show that the distance to the rooted nodes within subgraphs is key to boosting their representation power. We then propose a structural embedding to encode such distance information.

(3) We propose a model, Efficient Substructure Counting GNN (ESC-GNN), which enhances a basic GNN with the structural embedding. It only needs to run message passing on the whole graph, and thus is much more efficient than subgraph GNNs. We evaluate ESC-GNN on various real-world and synthetic benchmarks. Experiments show that ESC-GNN performs comparably with subgraph GNNs on real-world tasks and counting substructures, while running much faster.

## 2 RELATED WORKS

### 2.1 Representation power of GNNs

There are two major perspectives to evaluate the representation power of GNNs: the ability to distinguish non-isomorphic graphs, and the ability to approximate specific functions. In terms of differentiating graphs, existing works [51, 73] showed that MPNNs are at most as powerful as 1-WL [69]. Following works improve the expressiveness of GNNs by using high-order information [10, 11, 45, 50, 51, 66, 68, 75] or augmenting node features [1, 6, 13, 15, 21, 36, 39, 40, 43, 48].

In terms of approximating specific functions, some works use GNNs to approximate graph algorithms [65, 72, 77] or detect bi-connectivity [83]. In this paper, we focus on counting substructures. Previous works [3, 25] relate the counting power to the expressiveness of GNNs. Following works count substructures with globally expressive networks [16, 52, 64] that are with high computational

costs. Several other works [41, 42, 82] also focus on counting substructures. However, they do not provide theoretical guarantees for these counts. Therefore we cannot trust their performance on substructure-related tasks, which are abundant in chemistry and biology.

### 2.2 Subgraph GNNs

Subgraph GNNs can be divided according to their subgraph selection policies, such as graph element deletion [9, 18, 54], k-hop subgraph extraction [2, 23, 53, 62, 79], node identity augmentation [81], and rooted subgraph extraction [8, 24, 30, 55, 58, 78, 84–87]. Most subgraph GNNs need to run message passing over all subgraphs, therefore performing much slower than classic MPNNs. This prevents their use in large real-world datasets.

### 2.3 Positional/Structural Encodings on Graphs

To leverage the spectral properties of graphs, many works [20, 21, 36, 40, 47, 56, 60] introduce the eigenvectors of the graph Laplacian as augmented node features. Other approaches introduce encodings with essential graph features [13, 22, 29, 33, 38, 67, 74, 76, 80, 89, 90]. Our work can be viewed as a subgraph-based structural encoding.

## 3 PRELIMINARIES

Let  $G = (V, E)$  be a simple, undirected graph, where  $V = \{1, 2, \dots, N\}$  is the node set, and  $E$  is the edge set. We use  $x_v$  to represent the node attribute for  $v \in V$ , and  $e_{uv}$  to represent the edge attribute for  $uv \in E$ . Denote the  $h$ -hop neighborhood of node  $v$  as  $V_v^h = \{u \in V \mid d(u, v) \leq h\}$ , where  $d(u, v)$  denotes the shortest path distance between node  $u$  and  $v$ . For a special case where  $h = 1$ , we call it the neighborhood of node  $v$ :  $N(v) = V_v^1$ .

Define a subgraph of  $G$  as any graph  $G^S = (V^S, E^S)$  with  $V^S \subseteq V$  and  $E^S \subseteq E$ . And an induced subgraph of  $G$  is any graph  $G^I = (V^I, E^I)$  where  $V^I \subset V$ , and  $E^I = E \cap (V^I)^2$  is the set of all edges in  $E$  where both nodes belong to  $V^I$ . For a  $k$ -tuple  $\vec{v} = (v_1, \dots, v_k) \in (V)^k$ , define its rooted  $h$ -hop subgraph as  $G_{\vec{v}}^h = (V_{\vec{v}}^h, E_{\vec{v}}^h)$ , where  $V_{\vec{v}}^h$  is the union of the  $h$ -hop neighborhoods of all vertices in  $\vec{v}$ :  $V_{\vec{v}}^h = V_{v_1}^h \cup \dots \cup V_{v_k}^h$ , and  $E_{\vec{v}}^h = E \cap (V_{\vec{v}}^h)^2$  are edges whose two nodes both belong to  $V_{\vec{v}}^h$ . Later, We will omit the hop parameter  $h$  for simplicity.

In this paper, we focus on graph-level counting of connected substructures<sup>1</sup>. Connected substructures are substructures whose nodes belong to a connected component. We study four types of connected substructures that are widely used in existing works: cycles, cliques, stars, and paths. An  $L$ -path is a sequence of edges  $[(v_1, v_2), \dots, (v_L, v_{L+1})]$  such that all nodes are distinct; an  $L$ -cycle is an  $L$ -path except that  $v_1 = v_{L+1}$ ; an  $L$ -clique is a fully connected graph with  $L$  nodes; and an  $L$ -star denotes a set of edges  $[(v, v_1), (v, v_2), \dots, (v, v_{L-1})]$  where all nodes with different symbols are distinct. Two substructures are called equivalent if their sets of edges are equal. Given a substructure  $S$  and a graph  $G$ , the **subgraph counting** is defined as counting the number of inequivalent substructures  $C_S(S, G)$  that are subgraphs of  $G$ . The **induced subgraph counting** is defined as counting the number of inequivalent

<sup>1</sup>Some works [30] focus on node-level counting, which can also be transferred to graph-level counting.

substructures that are induced subgraphs of  $G$ . In this paper, we focus on subgraph counting, but we also provide theoretical results on induced subgraph counting.

Following existing works [16, 30], we formally define substructure counting as:

**Definition 3.1.** Let  $\mathcal{G}$  be the set of all graphs and  $\mathcal{F}$  be a function class over graphs. We say  $\mathcal{F}$  can count connected substructure  $S$  on  $\mathcal{G}$  if for all  $G_1, G_2 \in \mathcal{G}$  such that  $C_S(S, G_1) \neq C_S(S, G_2)$ , their exists  $f \in \mathcal{F}$  that  $f(G_1) \neq f(G_2)$ .

Using the Stone-Weierstrass theorem, the definition is equivalent to approximating subgraph-counting functions [16]. If replacing  $C_S$  by  $C_I$ , then the task will be naturally turned to induced subgraph counting.

## 4 COUNTING POWER OF SUBGRAPH GNNs

Subgraph GNNs have been proven to possess the capability to count specific substructures [16, 30, 81, 87]. We commence by introducing subgraph GNNs in Section 4.1. In Section 4.2, we characterize the general substructure counting power of subgraph GNNs, by proving that they are nearly as powerful as globally expressive models while running much faster. We theoretically show that the distance information within the subgraph is key to boosting the counting power of GNNs. Such information can be encoded into a structural embedding, providing the basis for our proposed efficient substructure-counting model<sup>2</sup>.

### 4.1 Subgraph GNNs

In this section, we introduce subgraph GNNs and refer readers to the appendix for details on the Weisfeiler-Leman algorithm (WL) [69] and MPNNs.

Subgraph GNNs first represent the input graph by a collection of subgraphs based on certain subgraph selection policies. They then encode the subgraphs using backbone GNNs and aggregate subgraph representations into the graph representation. We note that there exist some other variants of subgraph GNNs [9, 24, 58, 87], but in this paper, we focus on a specific type of subgraph GNNs without information exchange between subgraphs, which covers reconstruction GNNs [18, 54], ID-GNNs [81], and nested GNNs [30, 85]. We will show that this type of subgraph GNNs is powerful enough in terms of counting connected substructures.

We call their subgraph selection policy as *rooted subgraph extraction policy*. Existing works select subgraphs rooted at either nodes [81, 85] or  $k$ -tuples [30, 58], and typically use a 1-WL equivalent GNN as the backbone. In this paper, we propose a more general framework with  *$m$ -WL (or its equivalent GNN) as the backbone on subgraphs rooted at connected  $k$ -tuples*, i.e.,  $k$ -tuples in which their induced subgraphs are connected. For a connected  $k$ -tuple  $\vec{v}$ , the selected subgraph is its rooted subgraph  $G_{\vec{v}} = (V_{\vec{v}}, E_{\vec{v}})$ .

Denote  $c_{\vec{v}, \vec{u}}^t$  as the color for an  $m$ -tuple  $\vec{u} = (u_1, \dots, u_m)$  in  $G_{\vec{v}}$  at iteration  $t$ . It is computed by:

$$c_{\vec{v}, \vec{u}}^t = \text{HASH}(c_{\vec{v}, \vec{v}}^{t-1}, c_{\vec{v}, \vec{u}}^{t-1}, c_{\vec{v}, \vec{u}, (1)}^t, \dots, c_{\vec{v}, \vec{u}, (k)}^t) \quad (1)$$

<sup>2</sup>The distance-related information also strongly influences the expressiveness of subgraph GNNs since the subgraph selection policies and the unsymmetric treatment to the rooted node and other nodes are both based on such information.

where

$$c_{\vec{v}, \vec{u}, (i)}^t = \{\{c_{\vec{v}, \vec{q}}^{t-1} | \vec{q} \in N_{\vec{v}, i}(\vec{u})\}, i \in [m] \quad (2)$$

Here  $N_{\vec{v}, i}(\vec{u}) = \{(u_1, \dots, u_{i-1}, w, u_{i+1}, \dots, u_m) | w \in V_{\vec{v}}\}$  denotes the  $i$ -th neighborhood of  $\vec{u}$  in  $G_{\vec{v}}$ .

Denote the final iteration as iteration  $T$ . The color of  $\vec{v}$  after the final iteration will be the combination of all  $m$ -tuples' colors inside  $G_{\vec{v}}$ . Formally,

$$c_{\vec{v}} = \text{Readout}(\{\{c_{\vec{v}, \vec{u}}^T | \vec{u} \in (V_{\vec{v}})^m\}\}) \quad (3)$$

where *Readout* is a readout function, e.g., the sum function. Intuitively, compared with MPNNs, subgraph GNNs (1) update the representation using not only the neighboring information but also the information from the rooted nodes; (2) the neighborhood is restricted to the subgraph level.

### 4.2 Counting Power of Subgraph GNNs

Subgraph GNNs possess the ability to count substructures. Existing works mainly focus on counting certain types of substructures, e.g., walks [81] and cycles [30] and do not relate subgraph GNNs with substructure counting in a holistic perspective. In this section, we characterize the general substructure counting power of subgraph GNNs by showing that they are nearly as powerful as globally expressive models, e.g., high-dimensional WL, while running much faster. We first theoretically characterize  $m$ -WL's power for counting **any** substructures.

**Counting power of  $m$ -WL.** Different substructures with no more than  $m$  nodes have different initial isomorphic types. We can assign each isomorphic type a unique color, and define the color histogram of the graph as the output function. Therefore the lower bound of the counting power of  $m$ -WL is:

*Remark 4.1.*  $m$ -WL ( $m \geq 2$ ) can count all connected substructures with no more than  $m$  nodes.

As for the upper bound, we show that for any  $m \geq 2$ , there exists a type of connected substructure with  $m+1$  nodes that  $m$ -WL cannot count. The theorem is formally stated below, and the proofs of the following theorems are provided in the appendix.

**Theorem 4.2.** *For any  $m \geq 2$ , there exists a pair of graphs  $G$  and  $H$ , such that  $G$  contains an  $(m+1)$ -clique as its subgraph while  $H$  does not, and that  $m$ -WL cannot distinguish  $G$  from  $H$ .*

Theorem 4.2 makes the lower bound in Remark 4.1 tight.

**Decomposition of counting connected substructures.** Before discussing the counting power of subgraph GNNs, we first provide the basis for the discussion: any graph-level substructure counting can be naturally decomposed into a collection of local substructure counting. For example, to count 3-cliques/3-cycles in a given graph, we can first compute the number of 3-cycles that pass each node, sum the number among all nodes, and then divide the number by  $3^3$  to compute the graph-level result. We can extend the observation to a more general version:

*Remark 4.3.* To count a certain type of connected substructures with no more than  $m+k$  ( $m \geq 2, k > 0$ ) nodes in a given graph, we can decompose it into counting over  $k$ -tuples. First, select a specific

<sup>3</sup>This number is strongly related to graph automorphism and is specific to the type of structure.

type of connected  $k$ -tuple whose induced subgraph is a subgraph of the target substructure. Then count the substructures that pass each  $k$ -tuple. Finally, the result is the sum of the numbers over all  $k$ -tuples divided by a constant dependent on the substructure.

**Counting power of subgraph GNNs.** We first give the lower bound below.

**Theorem 4.4.** *For any connected substructure with no more than  $m + k$  ( $m \geq 2, k > 0$ ) nodes, there exists a subgraph GNN rooted at  $k$ -tuples with backbone GNN as powerful as  $m$ -WL that can count it.*

Based on the proof and the insights gained from popular subgraph GNNs, we can safely conclude that *the distance from the rooted nodes to nodes within the subgraph provides valuable information for substructure counting*. As for the upper bound of the counting power of subgraph GNNs, existing works [24, 26] show that for  $m \geq 2$ , (1)  $m$ -WL is as powerful as a specific GNN, called  $m$ -IGN [46]; (2) a subgraph GNN rooted at  $k$ -tuple with backbone GNN as powerful as  $m$ -WL can be implemented by a  $(m + k)$ -IGN (which can be easily induced by Lemma 5 in [24]). Therefore, we have:

*Remark 4.5.* Any subgraph GNN rooted at  $k$ -tuples with backbone GNN as powerful as  $m$ -WL ( $m \geq 2$ ) is not more powerful than  $(m + k)$ -WL.

Combining with Theorem 4.2, we obtain a tight characterization of subgraph GNNs' counting power for any substructures, which is the same as  $(m + k)$ -WL. This suggests that subgraph GNNs are nearly as powerful as globally expressive models in terms of graph-level general substructure counting. Note that globally expressive models might still be more powerful at counting specific substructures.

**Efficiency of subgraph GNNs.** The computational cost for  $(m + k)$ -WL is  $O(|V|^{m+k})$ , where  $|V|$  denotes the number of nodes in the input graph. However, for subgraph GNNs rooted at  $k$ -tuples with backbone GNN as powerful as  $m$ -WL, the computational cost can be  $O(|V|^k |V_s|^m)$ , where  $V_s$  is the largest number of nodes among all subgraphs. We point out that  $|V_s|$  is usually much smaller than  $|V|$ . For example, when counting cliques and stars, the hop parameter can be set to 1; when counting cycles and paths, the hop parameter can be set to  $m/2$ . Therefore subgraph GNNs are much more efficient. In conclusion, subgraph GNNs rooted at  $k$ -tuples with backbone GNN as powerful as  $m$ -WL can reach a similar counting power to  $(m + k)$ -WL while being much more efficient. This can be a key motivation for the use of subgraph GNNs in counting substructures.

## 5 EFFICIENT SUBSTRUCTURE COUNTING GNN (ESC-GNN)

Despite the strong substructure counting ability, subgraph GNNs are still much slower than MPNNs since they need to run backbone GNNs on all subgraphs. In this section, we propose a model, Efficient Substructure Counting GNN (ESC-GNN), which can count substructures efficiently and effectively, while, more importantly, does not need to run GNN on subgraphs. ESC-GNN encodes the distance information within subgraphs into structural embeddings of edges in a preprocessing step. After that, it only needs to **run**

**the backbone GNN on the input graph once rather than over all subgraphs**. We first introduce ESC-GNN, and then show its representation power theoretically.

### 5.1 Framework of ESC-GNN

**Basic framework.** In this section, we first introduce the framework of ESC-GNN, which is illustrated in Figure 1. In ESC-GNN, we adopt subgraphs rooted at 2-tuples, and use MPNN as the backbone GNN. Subgraph GNNs rooted at 2-tuples are more expressive than those rooted at nodes, but at the cost of even higher computational cost [30]. Thus, instead of running backbone GNN over subgraphs to extract subgraph features (like distances), we directly encode them into some carefully designed structural embeddings, which are used as additional edge features of the input graph. An MPNN is then applied to this augmented graph. Specifically, let  $h_v^t$  be the node representation for  $v \in V$  in the  $t$ -th iteration. The update function is given by:

$$h_v^{t+1} = W_1^t(h_v^t, \sum_{u \in \mathcal{N}(v)} W_2^t(h_u^t, h_v^t, e_{uv}, s_{uv})) \quad (4)$$

where  $s_{uv}$  is the structural embedding for edge  $uv$ .

**Choice of structural embedding.** Recall the proof of Theorem 4.4 and the statement in Section 4 imply that the distance information within subgraphs is key to boosting the counting power of subgraph GNNs. Therefore, we encode such distance information, as well as some degree information, which provides the information of isomorphic types, as follows. An example is shown in Figure 1.

- The degree encoding: for each subgraph, we first compute the degree of all nodes within the subgraph, and then use the degree histogram as the encoding. For example, the degree histogram for the first subgraph (the subgraph rooted at edge  $v_1v_3$ ) of Figure 1 is  $(0, 0, 4, 0)$ , since there are 4 nodes with degree 2 in the subgraph.
- The node-level distance encoding: for the subgraph rooted at edge  $uv$ , we use the shortest path distance histograms to the rooted nodes as the distance encoding. Take the first subgraph of Figure 1 as an example. The distance histogram for  $v_1$  is  $(1, 2, 1, 0)$ , since there are one node with distance 0 ( $v_1$ ), two nodes with distance 1 ( $v_2$  and  $v_3$ ), and one node with distance 2 ( $v_4$ ) to node  $v_1$ . The same holds for the other rooted node  $v_3$ .
- The edge-level distance encoding: for the subgraph rooted at edge  $uv$ , define the label for each node as its shortest path distances to all the rooted nodes, i.e.,  $\forall u_1, f(u_1) = (d(u_1, u), d(u_1, v))$ . Then we can define the label of edges in the subgraph as the concatenation of the label of its two end nodes, e.g., for edge  $u_1v_1$ , its label is  $f(u_1v_1) = (f(u_1), f(v_1))$ . We then use the edge-level distance histogram as the distance encoding. For example, for the subgraphs shown in Figure 1, there are seven types of edges:  $(0,1,1,0)$ ,  $(0,1,1,1)$ ,  $(0,1,1,2)$ ,  $(1,0,1,1)$ ,  $(1,0,2,1)$ ,  $(1,2,2,1)$ ,  $(2,1,2,1)$ . Therefore the edge-level distance encoding for the first subgraph is  $(1,0,1,0,1,1,0)$ , since there are one edge ( $v_1v_3$ ) with label  $(0,1,1,0)$ , one edge ( $v_1v_2$ ) with label  $(0,1,1,2)$ , one edge ( $v_3v_4$ ) with label  $(1,0,2,1)$ , and one edge ( $v_2v_4$ ) with label  $(1,2,2,1)$ .

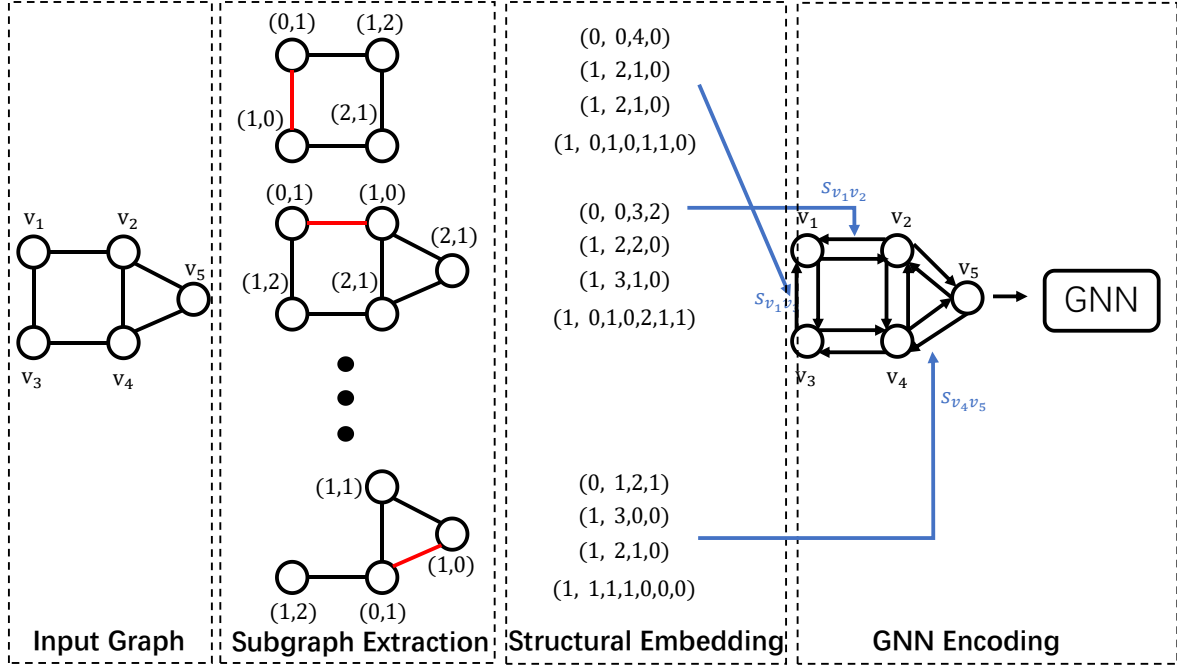


Figure 1: Framework of ESC-GNN. The rooted 2-tuples are colored red during subgraph extraction.

Finally, we concatenate the three encodings to get the final structural embedding  $s_{uv}$ .

**Analysis on the structural embedding.** In terms of representation power, we find that (1) all these distance encodings can be extracted using an MPNN within the subgraph, (2) subgraph MPNNs rooted at 2-tuple can count structures such as 5-cycles [30], while ESC-GNN cannot. Consequently, based on these considerations, we arrive at the following conclusion:

**Proposition 5.1.** *ESC-GNN is less powerful than subgraph GNNs rooted at 2-tuples with MPNN as the backbone GNN.*

In terms of algorithm efficiency, we can precompute these structural embeddings during subgraph extraction (the preprocessing cost can be amortized into each epoch/iteration), and ESC-GNN only needs to run the backbone GNN on the input graph. Therefore in every iteration, its computational cost is only  $O(|E|)$ , and its memory cost is  $O(|V|)$ , both the same as MPNN. As for subgraph MPNNs rooted at edges, they need to run the process of subgraph extraction and run the backbone GNN over all subgraphs. In every iteration, their computational cost is  $O(|E||E'_s|)$ , and their memory cost is  $O(|E||V'_s|)$ , where  $|V'_s|$  and  $|E'_s|$  are the average numbers of nodes and edges among all subgraphs. Even if considering subgraph MPNNs rooted at nodes, in every iteration, their computational cost is  $O(|V||E_s|)$ , and their memory cost is  $O(|V||V_s|)$ . Note that  $|V||E_s| \gg \frac{|V|D}{2} = |E|$ , where  $D$  is the average node degree. Therefore we can safely conclude that ESC-GNN is more efficient than subgraph GNNs. We will empirically evaluate its efficiency in the experiment.

## 5.2 Representation Power of ESC-GNN

In this section, we analyze the representation power of ESC-GNN from two perspectives: its counting power and its ability to distinguish non-isomorphic graphs.

**Counting power of ESC-GNN.** Existing works [30, 81] mainly focus on subgraph counting. Here we provide results on both subgraph counting and induced subgraph counting. We use four popular types of substructures: cycles, cliques, stars, and paths, as examples to show the counting power of ESC-GNN. The proof is provided in the appendix.

**Theorem 5.2.** *In terms of subgraph counting, ESC-GNN can count (1) up to 4-cycles; (2) up to 4-cliques; (3) stars with arbitrary sizes; (4) up to 3-paths.*

**Theorem 5.3.** *In terms of induced subgraph counting, ESC-GNN can count (1) up to 4-cycles; (2) up to 4-cliques; (3) up to 4-stars; (4) up to 3-paths.*

**Compared with subgraph GNNs.** As shown in Proposition 5.1, ESC-GNN is less powerful than subgraph MPNNs rooted at 2-tuples [30]. As for subgraph MPNNs rooted at nodes [81, 85], they can only count up to 4-cycles, 3-cliques, and 3-paths [30]. Therefore, ESC-GNN is more powerful than subgraph MPNNs rooted at nodes in terms of counting these substructures.

**From graph-level substructure counting to node-level substructure counting.** It is important to recognize that counting substructures at the graph level presents a lesser challenge compared to node-level substructure counting. The reason behind this is straightforward: the total number of substructures within a graph can be computed through the weighted sum of the counts of substructures passing each node. Conversely, the inverse process is

not inherently feasible. Although our proof predominantly concentrates on graph-level counting, its principles bear the potential for adaptation to node-level counting scenarios.

To illustrate this concept, consider a structure  $s$ . Let  $n_{uv}$  denotes the number of  $s$  that passes the 2-tuple  $(u, v)$ , and let  $p$  denotes the number of automorphisms of the 2-tuple starting at node  $u$ . In other words,  $p$  quantifies the number of 2-tuples starting from  $u$  that mirror the isomorphic type of  $(u, v)$  within structure  $s$ . Consequently, the aggregate count of structure  $s$  that passes node  $u$  is  $\sum_{v \in N(u)} n_{uv}/k$ . Take the counting of 3-cycles  $s = \{u, v, w\}$  that passes node  $u$  as an example.  $k$  is 2 since in  $s$ , both  $(u, v)$  and  $(u, w)$  have the same isomorphic type as  $(u, v)$  ( $(u, w)$ , resp.). Considering that there is a cycle that passes  $(u, v)$  ( $(u, w)$ , resp.), the number of 3-cycles that passes  $u$  is  $(1 + 1)/2 = 1$ .

**The ability to distinguish non-isomorphic graphs.** In terms of distinguishing non-isomorphic graphs, we present the result below:

**Theorem 5.4.** *ESC-GNN is strictly more powerful than 2-WL, while not less expressive than 3-WL.*

**Compared with subgraph GNNs.** In terms of distinguishing non-isomorphic graphs, subgraph MPNNs rooted at nodes [81, 85] are strictly less powerful than 3-WL [24], while ESC-GNN is not less expressive than 3-WL.

In addition, although able to distinguish most pairs of non-isomorphic graphs [4], 2-WL fails to distinguish any pairs of non-isomorphic  $r$ -regular graphs with equal size. In this paper, we prove that ESC-GNN can distinguish almost all  $r$ -regular graphs:

**Theorem 5.5.** *Consider all pairs of  $r$ -regular graphs with  $n$  nodes, let  $3 \leq r < (2 \log 2n)^{1/2}$  and  $\epsilon$  be a fixed constant. With the hop parameter  $h$  set to  $\lfloor (1/2 + \epsilon) \frac{\log 2n}{\log(r-1)} \rfloor$ , there exists an ESC-GNN that can distinguish  $1 - o(n^{-1/2})$  such pairs of graphs.*

Furthermore, we also show that ESC-GNN’s representation power also benefits from its global message passing layer in Section H in the appendix.

## 6 EXPERIMENT

To thoroughly analyze the property of ESC-GNN, we evaluate it from the following perspectives: (1) we evaluate its representation power in Section 6.1, to show whether it can reach the theoretical power shown in Section 5.2; (2) we evaluate its performance on real-world benchmarks in Section 6.2, to show whether the increased representation power can boost its performance on real-world tasks; (3) we evaluate its efficiency in Section 6.3. The code is available at <https://github.com/pkuyzy/ESC-GNN>.

We provide the experimental details, the analysis on the limitation of the paper, and the information of the used assets in the appendix.

**Baselines.** We compare with baseline methods including (1) basic MPNNs [34, 73]; (2) subgraph GNNs including NGNN [85], IDGNN [81], GIN-AK+ [87], SUN [24], DSS-GNN [9], OSAN [58], I<sup>2</sup>-GNN [30], and PL-GNN [8]; (3) high-order GNN models including 1-2-3-GNN [51] and PPGN [45]; (4) graph transformers including Graphormer-GD [83] and GraphGPS [60]; and (5) GNNs that incorporate the substructure information, including LGP-GNN [6] and GSN [13].

### 6.1 Representation Power of ESC-GNN

**Datasets.** We evaluate the representation power of ESC-GNN from two perspectives:

(a) Its ability to differentiate non-isomorphic graphs. We use (1) EXP [1], which contains 600 pairs of non-isomorphic graphs that 1-WL/2-WL fails to distinguish; (2) SR25 [5], which contains 150 pairs of non-isomorphic strongly regular graphs that cannot be differentiated by 3-WL; (3) CSL [52], which contains 150 regular graphs that 1-WL/2-WL fails to distinguish. These graphs are classified into 10 isomorphism classes. Classification accuracy is adopted as the evaluation metric.

(b) Its counting ability. We use the synthetic dataset from [87]. The task is to predict the number of substructures that pass each node in the given graph. The Mean Absolute Error (MAE) is adopted as the evaluation metric.

**Results.** In Table 2, ESC-GNN achieves 100% accuracy on all datasets. Considering that models as powerful as 3-WL (PPGN and 3-GNN) fail the SR25 dataset, the results serve as empirical evidence that ESC-GNN can effectively differentiate regular graphs (Theorem 5.5), and not less powerful than 3-WL (Theorem 5.4). In Table 1, ESC-GNN reaches less-than-0.01 MAE in terms of counting tailed triangles, 4-cliques, 3-cycles, and 4-cycles. The low error allows us to simply apply a rounding function to obtain the ground truth integer counting results, thus are considered an indicator of successful counting as in previous works [30]. These counting results exactly match Theorem 5.2. Generally speaking, ESC-GNN performs much better than MPNNs, and slightly beats or performs comparably with node-based subgraph GNNs such as ID-GNN, NGNN and GIN-AK+. Also, it performs inferior to subgraph GNNs rooted at edges (I<sup>2</sup>-GNN). This serves as the empirical evidence for Proposition 5.1. In addition, graph transformers such as GraphGPS<sup>4</sup> and Graphormer-GD have shown impressive performance in previous studies, particularly on graph-level prediction tasks. However, they perform inferior to subgraph GNNs and our proposed model on the substructure-counting task. This observation suggests potential limitations in the applicability of these transformer-based models to tasks involving substructure analysis.

### 6.2 Real-World Tasks

We present our experiments conducted on datasets including QM9 [59, 71], OGBG-MOLHIV [28], and ZINC [20]. These results are reported in Table 4 and Table 5. On QM9 and ZINC, the task is to perform regression on various graph properties. While on OGBG-MOLHIV, the task is to predict the classification of molecule graphs. Detailed statistics are available in Section J in the appendix.

**Comparison with backbone models.** On OGBG-MolHIV and QM9, we use GIN [73] as the backbone model. While on ZINC, we use a **plain graph transformer without positional encodings** from [60] as the backbone model. The comparison between ESC-GNN and the backbone models demonstrates that the proposed structural information not only enhances the theoretical representation power but also improves the empirical representation power.

**Comparison with subgraph GNNs.** When compared to subgraph GNNs, such as PL-GNN, OSAN, DSS-GNN, I<sup>2</sup>-GNN, NGNN,

<sup>4</sup>We exclude the laplacian-based structural embeddings since they are not permutation-invariant, i.e., they may produce different outputs for the same graph.

**Table 1: Evaluation on Counting Substructures (norm MAE), cells with MAE less than 0.01 (an indicator of successful counting [30]) are colored yellow.**

Dataset	Tailed Triangle	Chordal Cycle	4-Clique	4-Path	Triangle-Rectangle	3-cycles	4-cycles	5-cycles	6-cycles
MPNN	0.3631	0.3114	0.1645	0.1592	0.2979	0.3515	0.2742	0.2088	0.1555
ID-GNN	0.1053	0.0454	0.0026	0.0273	0.0628	0.0006	0.0022	0.0490	0.0495
NGNN	0.1044	0.0392	0.0045	0.0244	0.0729	0.0003	0.0013	0.0402	0.0439
GIN-AK+	0.0043	0.0112	0.0049	0.0075	0.1311	0.0004	0.0041	0.0133	0.0238
PPGN	0.0026	0.0015	0.1646	0.0041	0.0144	0.0005	0.0013	0.0044	0.0079
I <sup>2</sup> -GNN	0.0011	0.0010	0.0003	0.0041	0.0013	0.0003	0.0016	0.0028	0.0082
Graphormer-GD	0.3660	0.2611	0.1580	0.1125	0.2460	0.3080	0.2317	0.1540	0.1380
GraphGPS	0.0132	0.0630	0.1156	0.0910	0.0551	0.0882	0.1645	0.0462	0.1193
ESC-GNN	0.0052	0.0169	0.0064	0.0254	0.0178	0.0074	0.0044	0.0356	0.0337

**Table 2: Test Accuracy on EXP/SR25/CSL**

Dataset	EXP	SR25	CSL
MPNN	50	6.67	10
NGNN	100	6.67	-
GIN-AK+	100	6.67	-
PPGN	100	6.67	-
3-GNN	99.7	6.67	95.7
I <sup>2</sup> -GNN	100	100	100
ESC-GNN	100	100	100

**Table 3: Evaluation on Algorithm Efficiency on OGBG-HIV (Seconds).**

Model	Pre	Run
MPNN	2.7	6296.8
NGNN	1288.0	14862.9
I <sup>2</sup> -GNN	2806.5	1042963.7
GIN-AK+(Sample)	376.2	10275
OSAN (Sample)	6.6	7980.1
ESC-GNN	1782.5	6301.0

**Table 4: Evaluation on QM9 (MAE)**

Dataset	1-GNN	1-2-3-GNN	NGNN	I <sup>2</sup> -GNN	ESC-GNN
$\mu$	0.493	0.476	0.428	0.428	<b>0.231</b>
$\alpha$	0.78	0.27	0.29	<b>0.230</b>	0.265
$\epsilon_{\text{homo}}$	0.00321	0.00337	0.00265	0.00261	<b>0.00221</b>
$\epsilon_{\text{lumo}}$	0.00355	0.00351	0.00297	0.00267	<b>0.00204</b>
$\Delta_{\epsilon}$	0.0049	0.0048	0.0038	0.0038	<b>0.0032</b>
$R^2$	34.1	22.9	20.5	18.64	<b>7.28</b>
ZPVE	0.00124	0.00019	0.0002	<b>0.00014</b>	0.00033
$U_0$	2.32	0.0427	0.295	<b>0.211</b>	0.645
$U$	2.08	<b>0.111</b>	0.361	0.206	0.380
$H$	2.23	<b>0.0419</b>	0.305	0.269	0.427
$G$	1.94	<b>0.0469</b>	0.489	0.261	0.384
$C_v$	0.27	0.0944	0.174	<b>0.0730</b>	0.105

and GIN-AK+, ESC-GNN parallels or slightly surpasses these models on these benchmarks. This finding substantiates that the proposed structural embedding effectively captures valuable information from subgraph GNNs, thereby benefiting downstream tasks. Moreover, the framework of ESC-GNN is simple enough to avoid problems such as overfitting. However, it is noteworthy that ESC-GNN’s performance on  $U_0$ ,  $U$ , and  $H$  in Table 4—representing Internal Energy at 0K, Internal Energy at 298.15K, and Enthalpy at 298.15K, respectively—does not reach optimal levels. To calculate these targets, computational methods take into account the interactions between all the atoms in the molecule and their surroundings, including any heat or work exchanged with the environment. As a result, globally expressive models (such as 1-2-3 GNN) exhibit superior performance, while subgraph GNNs, which utilize local information to enhance graph representation, show relatively diminished efficacy.

In terms of OGBG-HIV, although ESC-GNN outperforms the majority of subgraph GNNs, it performs inferior to the state-of-the-art (SOTA) models. This phenomenon could be attributed to the intricate nature of HIV replication inhibition, which is governed by a complex interplay of both local and global attributes. Specifically, local attributes include the structure and functionality of specific molecules and their enzymatic active sites, while global attributes encompass the overarching graph structure of both the viral components and the molecular constituents within cellular matrices and their interactive cross-sections.

Consequently, SOTA models combine global information — such as graph pooling models, high-order message passing techniques, or graph transformers — with local information. An example of the latter is the molecular fingerprint, which encapsulates the count of various specific molecules particular to specific domains. While these fingerprints offer detailed insights, there is a notable risk of overfitting when applied to certain datasets, potentially limiting their generalizability and applicability in broader contexts.

**Comparison with GNNs that incorporate the substructure information.** GSN [13] and LGP-GNN [6] incorporate the number of specific substructures as augmented features. The approach heavily relies on domain-specific knowledge and the desired substructures may significantly vary across different tasks. In contrast, our ESC-GNN framework does not explicitly encode the number of substructures. Instead, it encodes the more general distance information of subgraphs, which enables plain GNNs to implicitly count

**Table 5: Evaluation on ZINC and OGB datasets.**

Dataset	OGBG-HIV (AUCROC)	ZINC-250K (MAE)	ZINC-12K (MAE)
GIN [73]	77.07±1.49	0.088±0.002	0.163±0.004
PNA [17]	79.05±1.32	-	0.188±0.004
GSN [13]	77.99±0.01	-	0.115±0.012
LGP-GNN [6]	-	-	0.135±0.010
DGN [7]	79.70±0.97	-	0.168±0.003
CIN [10]	<b>80.94±0.57</b>	0.022±0.002	0.079±0.006
NGNN [85]	78.34±1.86	0.029±0.001	0.111±0.003
GIN-AK+ [87]	79.61±1.19	-	0.080±0.001
OSAN [58]	78.01±1.04	-	0.126±0.006
SUN [24]	80.03±0.55	-	0.083±0.003
DSS-GNN [9]	76.78±1.66	-	0.102±0.003
I <sup>2</sup> -GNN [30]	78.68±0.93	0.023±0.001	0.083±0.001
PL-GNN [8]	78.49±1.01	-	0.109±0.005
Graph Transformer [60]	77.40±1.77	0.030±0.006	0.113±0.003
ESC-GNN	79.21±0.84	<b>0.021±0.003</b>	<b>0.075±0.002</b>

**Table 6: Ablation study on the proposed structural embedding (norm MAE).**

Dataset	Tailed Triangle	Chordal Cycle	4-Clique	4-Path	Triangle-Rectangle	3-cycles	4-cycles	5-cycles	6-cycles
MPNN	0.3631	0.3114	0.1645	0.1592	0.2979	0.3515	0.2742	0.2088	0.1555
ESC-GNN	<b>0.0052</b>	0.0169	<b>0.0064</b>	0.0254	0.0178	<b>0.0074</b>	<b>0.0044</b>	0.0356	0.0337
(- degree)	0.0121	0.0492	0.0106	0.0322	0.0349	0.0342	0.0144	0.0513	0.0652
(- node-level dist)	0.0382	0.0344	0.0222	0.0428	0.0256	0.0157	0.0261	0.0492	0.0608
(- edge-level dist)	0.0208	0.2811	0.0497	0.0584	0.185	0.2617	0.2244	0.1654	0.1364

many substructures without pre-selecting which to include. The general distance information contains more structural information than the number of specific substructures. For instance, we have proven that the number of 4-cycles can be computed using the distance information. Conversely, deducing distance information solely from the count of 4-cycles is impracticable, given the multiplicity of configurations that can form a 4-cycle. The superiority is also justified by empirical evidence in Section I in the Appendix.

Regarding the real-world dataset in Table 5, GSN achieves a MAE score of 0.115 on ZINC, whereas ESC-GNN attains a MAE score of 0.075. Similarly, GSN records an AUCROC score of 77.99 on OGBG-HIV, whereas ESC-GNN demonstrates a higher AUCROC score of 79.21. These results clearly highlight the enhanced representation power of our proposed model.

### 6.3 Algorithm Efficiency

In terms of algorithm efficiency, we conduct a comparison between the ESC-GNN and five established baseline models: a baseline MPNN, NGNN, OSAN, and GIN-AK+ whose subgraphs are rooted at node, and I<sup>2</sup>-GNN whose subgraphs are rooted at 2-tuples. We accelerate the code of I<sup>2</sup>-GNN by implementing a parallel subgraph preprocessing strategy. We report the data preprocessing time and the standard running time for running 100 epochs on ogbg-hiv in Table 3. It is crucial to note that while the sampling strategies employed in OSAN and GIN-AK+ contribute to increased speed,

they lose the theoretical substructure counting ability. This limitation arises because substructures present in unsampled subgraphs remain uncounted, leading to a reduction in representation power and, consequently, diminished performance. For example, employing subgraph sampling in OSAN results in an AUC-ROC score of 75.96 on OGBG-HIV, which is significantly less than the 78.01 score reported in Table 5. Therefore, a direct comparison with our approach, which does not rely on such sampling strategies, may not be entirely fair.

Nevertheless, for the sake of a thorough analysis, we have included these comparative results in Table 3. As shown in the table, ESC-GNN exhibits a notable advantage in terms of total running time compared to subgraph GNNs, including those utilizing theoretically unsound sampling methods. This efficiency is attributed to the fact that preprocessing in our model is a one-time requirement, with the processed data being reusable across all subsequent training and inference stages. This finding aligns with our observations presented in Section 5.1, further validating the superior efficiency and effectiveness of ESC-GNN in handling graph data.

### 6.4 Ablation Study

We evaluate the effectiveness of each part of the proposed structural embedding on the substructure counting dataset. For the proposed three types of structural embedding, we delete one of them from the original structural embedding every time and report the results



in Table 6. We observe that after removing the three types of embedding, ESC-GNN performs worse compared with its original version, especially after removing the edge-level distance encoding. This is consistent with our theoretical results, where in Theorem 4.4, we show that the proposed structural embedding contains key information for the counting power of subgraph GNNs; in Theorem 5.2 and Theorem 5.3, we show that the edge-level distance information encodes the information of certain types of substructures.

## 7 CONCLUSION

The huge computational cost is associated with subgraph GNNs due to the requirement of running backbone GNNs among all subgraphs. To address this challenge and enable efficient substructure counting with GNNs, we theoretically show that the distance information within subgraphs is key to boosting the counting power of GNNs. We then encode this information into a structural embedding and enhance standard GNN models with this embedding, eliminating the need to learn representations over all subgraphs. Experiments on various benchmarks demonstrate that the proposed model retains the representation power of subgraph GNNs while running much faster. It can potentially enhance the utility of subgraph GNNs in a variety of applications that require efficient substructure counting.

## ACKNOWLEDGEMENT

The work of Zuoyu Yan, Liangcai Gao, and Zhi Tang is supported by the projects of National Science and Technology Major Project (2021ZD0113301) and National Natural Science Foundation of China (No. 62376012), which is also a research achievement of Key Laboratory of Science, Technology and Standard in Press Industry (Key Laboratory of Intelligent Press Media Technology). The work of Junru Zhou and Muhan Zhang is supported by the National Natural Science Foundation of China (62276003), the National Key R&D Program of China (2021ZD0114702), and Alibaba Innovative Research Program.

## REFERENCES

- [1] Ralph Abboud, İsmail İlkan Ceylan, Martin Grohe, and Thomas Lukasiewicz. 2021. The Surprising Power of Graph Neural Networks with Random Node Initialization. In *Proceedings of the Thirtieth International Joint Conference on Artificial Intelligence, IJCAI 2021, Virtual Event / Montreal, Canada, 19-27 August 2021*, Zhi-Hua Zhou (Ed.). ijcai.org, 2112–2118. <https://doi.org/10.24963/IJCAI2021/291>
- [2] Sami Abu-El-Hajja, Bryan Perozzi, Amol Kapoor, Nazanin Alipourfard, Kristina Lerman, Hrayr Harutyunyan, Greg Ver Steeg, and Aram Galstyan. 2019. Mixhop: Higher-order graph convolutional architectures via sparsified neighborhood mixing. In *international conference on machine learning*. PMLR, 21–29.
- [3] Vikraman Arvind, Frank Fuhlbrück, Johannes Köbler, and Oleg Verbitsky. 2020. On Weisfeiler-Leman invariance: Subgraph counts and related graph properties. *J. Comput. System Sci.* 113 (2020), 42–59.
- [4] László Babai, Paul Erdos, and Stanley M Selkow. 1980. Random graph isomorphism. *Siam Journal on computing* 9, 3 (1980), 628–635.
- [5] Muhammet Balcilar, Pierre Héroux, Benoit Gauzere, Pascal Vasseur, Sébastien Adam, and Paul Honeine. 2021. Breaking the limits of message passing graph neural networks. In *International Conference on Machine Learning*. PMLR, 599–608.
- [6] Pablo Barceló, Floris Geerts, Juan Reutter, and Maksimilian Ryschkov. 2021. Graph neural networks with local graph parameters. *Advances in Neural Information Processing Systems* 34 (2021), 25280–25293.
- [7] Dominique Beaini, Saro Passaro, Vincent Létourneau, Will Hamilton, Gabriele Corso, and Pietro Liò. 2021. Directional graph networks. In *International Conference on Machine Learning*. PMLR, 748–758.
- [8] Eli Meirum Bruno Ribeiro Haggai Maron Beatrice Bevilacqua, Moshe Eliasof. 2024. Efficient Subgraph GNNs by Learning Effective Selection Policies. In *The Twelfth International Conference on Learning Representations*. <https://openreview.net/forum?id=gppLqZLQeY>
- [9] Beatrice Bevilacqua, Fabrizio Frasca, Derek Lim, Balasubramaniam Srinivasan, Chen Cai, Gopinath Balamurugan, Michael M Bronstein, and Haggai Maron. 2022. Equivariant Subgraph Aggregation Networks. In *International Conference on Learning Representations*.
- [10] Cristian Bodnar, Fabrizio Frasca, Nina Otter, Yuguang Wang, Pietro Lio, Guido F Montufar, and Michael Bronstein. 2021. Weisfeiler and Lehman go cellular: CW networks. *Advances in Neural Information Processing Systems* 34 (2021), 2625–2640.
- [11] Cristian Bodnar, Fabrizio Frasca, Yuguang Wang, Nina Otter, Guido F Montufar, Pietro Lio, and Michael Bronstein. 2021. Weisfeiler and Lehman go topological: Message passing simplicial networks. In *International Conference on Machine Learning*. PMLR, 1026–1037.
- [12] Béla Bollobás. 1982. Distinguishing vertices of random graphs. In *North-Holland Mathematics Studies*. Vol. 62. Elsevier, 33–49.
- [13] Giorgos Bouritsas, Fabrizio Frasca, Stefanos P Zafeiriou, and Michael Bronstein. 2022. Improving graph neural network expressivity via subgraph isomorphism counting. *IEEE Transactions on Pattern Analysis and Machine Intelligence* (2022).
- [14] Jin-Yi Cai, Martin Fürer, and Neil Immerman. 1992. An optimal lower bound on the number of variables for graph identification. *Combinatorica* 12, 4 (1992), 389–410.
- [15] Kaixuan Chen, Shunyu Liu, Tongtian Zhu, Ji Qiao, Yun Su, Yingjie Tian, Tongya Zheng, Hao-fei Zhang, Zunlei Feng, Jingwen Ye, and Mingli Song. 2023. Improving Expressivity of GNNs with Subgraph-specific Factor Embedded Normalization. In *Proceedings of the 29th ACM SIGKDD Conference on Knowledge Discovery and Data Mining (, Long Beach, CA, USA, (KDD '23)*. Association for Computing Machinery, New York, NY, USA, 237–249. <https://doi.org/10.1145/3580305.3599388>
- [16] Zhengdao Chen, Lei Chen, Soledad Villar, and Joan Bruna. 2020. Can graph neural networks count substructures? *Advances in neural information processing systems* 33 (2020), 10383–10395.
- [17] Gabriele Corso, Luca Cavalleri, Dominique Beaini, Pietro Liò, and Petar Velicković. 2020. Principal neighbourhood aggregation for graph nets. *Advances in Neural Information Processing Systems* 33 (2020), 13260–13271.
- [18] Leonardo Cotta, Christopher Morris, and Bruno Ribeiro. 2021. Reconstruction for powerful graph representations. *Advances in Neural Information Processing Systems* 34 (2021), 1713–1726.
- [19] Mukund Deshpande, Michihiro Kuramochi, and George Karypis. 2002. *Automated approaches for classifying structures*. Technical Report. MINNESOTA UNIV MINNEAPOLIS DEPT OF COMPUTER SCIENCE.
- [20] Vijay Prakash Dwivedi, Chaitanya K Joshi, Thomas Laurent, Yoshua Bengio, and Xavier Bresson. 2020. Benchmarking graph neural networks. *arXiv preprint arXiv:2003.00982* (2020).
- [21] Vijay Prakash Dwivedi, Anh Tuan Luu, Thomas Laurent, Yoshua Bengio, and Xavier Bresson. 2021. Graph Neural Networks with Learnable Structural and Positional Representations. In *International Conference on Learning Representations*.
- [22] Or Feldman, Amit Boyarski, Shai Feldman, Dani Kogan, Avi Mendelson, and Chaim Baskin. 2022. WEISFEILER AND LEMAN GO INFINITE: SPECTRAL AND COMBINATORIAL PRE-COLORINGS. In *ICLR 2022 Workshop on Geometrical and Topological Representation Learning*.
- [23] Jiarui Feng, Yixin Chen, Fuhai Li, Anindya Sarkar, and Muhan Zhang. 2022. How Powerful are K-hop Message Passing Graph Neural Networks. *arXiv preprint arXiv:2205.13328* (2022).
- [24] Fabrizio Frasca, Beatrice Bevilacqua, Michael M Bronstein, and Haggai Maron. 2022. Understanding and Extending Subgraph GNNs by Rethinking Their Symmetries. In *Advances in Neural Information Processing Systems*.
- [25] Martin Fürer. 2017. On the combinatorial power of the Weisfeiler-Lehman algorithm. In *International Conference on Algorithms and Complexity*. Springer, 260–271.
- [26] Floris Geerts. 2020. The expressive power of kth-order invariant graph networks. *arXiv preprint arXiv:2007.12035* (2020).
- [27] Martin Grohe and Martin Otto. 2015. Pebble Games and Linear Equations. *The Journal of Symbolic Logic* 80, 3 (2015), 797–844. <https://doi.org/10.1017/jsl.2015.28>
- [28] Weihua Hu, Matthias Fey, Marinka Zitnik, Yuxiao Dong, Hongyu Ren, Bowen Liu, Michele Catasta, and Jure Leskovec. 2020. Open graph benchmark: Datasets for machine learning on graphs. *Advances in neural information processing systems* 33 (2020), 22118–22133.
- [29] Yinan Huang, William Lu, Joshua Robinson, Yu Yang, Muhan Zhang, Stefanie Jegelka, and Pan Li. 2023. On the Stability of Expressive Positional Encodings for Graph Neural Networks. *arXiv preprint arXiv:2310.02579* (2023).
- [30] Yinan Huang, Xingang Peng, Jianzhu Ma, and Muhan Zhang. 2023. Boosting the Cycle Counting Power of Graph Neural Networks with IS<sup>2</sup>-GNNs. In *The Eleventh International Conference on Learning Representations*. <https://openreview.net/forum?id=kDSmxOspXQ>

- [31] Chuntao Jiang, Frans Coenen, and Michele Zito. 2010. Finding frequent subgraphs in longitudinal social network data using a weighted graph mining approach. In *International Conference on Advanced Data Mining and Applications*. Springer, 405–416.
- [32] Wengong Jin, Regina Barzilay, and Tommi Jaakkola. 2018. Junction tree variational autoencoder for molecular graph generation. In *International conference on machine learning*. PMLR, 2323–2332.
- [33] Nicolas Keriven and Samuel Vaiter. 2023. What functions can Graph Neural Networks compute on random graphs? The role of Positional Encoding. In *Thirty-seventh Conference on Neural Information Processing Systems*. <https://openreview.net/forum?id=Lmmj1TwYm0>
- [34] Thomas N. Kipf and Max Welling. 2017. Semi-Supervised Classification with Graph Convolutional Networks. In *5th International Conference on Learning Representations, ICLR 2017, Toulon, France, April 24–26, 2017, Conference Track Proceedings*. OpenReview.net. <https://openreview.net/forum?id=SJU4ayYgl>
- [35] Mehmet Koyutürk, Ananth Grama, and Wojciech Szpankowski. 2004. An efficient algorithm for detecting frequent subgraphs in biological networks. *Bioinformatics* 20, suppl\_1 (2004), i200–i207.
- [36] Devin Kreuzer, Dominique Beaini, Will Hamilton, Vincent Létourneau, and Prudencio Tossou. 2021. Rethinking graph transformers with spectral attention. *Advances in Neural Information Processing Systems* 34 (2021), 21618–21629.
- [37] P. Langley. 2000. Crafting Papers on Machine Learning. In *Proceedings of the 17th International Conference on Machine Learning (ICML 2000)*, Pat Langley (Ed.). Morgan Kaufmann, Stanford, CA, 1207–1216.
- [38] Pan Li, Yanbang Wang, Hongwei Wang, and Jure Leskovec. 2020. Distance encoding: Design provably more powerful neural networks for graph representation learning. *Advances in Neural Information Processing Systems* 33 (2020), 4465–4478.
- [39] Derek Lim, Joshua Robinson, Stefanie Jegelka, and Haggai Maron. 2023. Expressive Sign Equivariant Networks for Spectral Geometric Learning. In *Thirty-seventh Conference on Neural Information Processing Systems*. <https://openreview.net/forum?id=UWd4ysACo4>
- [40] Derek Lim, Joshua David Robinson, Lingxiao Zhao, Tess Smidt, Suvrit Sra, Haggai Maron, and Stefanie Jegelka. 2022. Sign and Basis Invariant Networks for Spectral Graph Representation Learning. In *ICLR 2022 Workshop on Geometrical and Topological Representation Learning*.
- [41] Xin Liu, Haojie Pan, Mutian He, Yangqiu Song, Xin Jiang, and Lifeng Shang. 2020. Neural subgraph isomorphism counting. In *Proceedings of the 26th ACM SIGKDD International Conference on Knowledge Discovery & Data Mining*, 1959–1969.
- [42] Xin Liu and Yangqiu Song. 2022. Graph Convolutional Networks with Dual Message Passing for Subgraph Isomorphism Counting and Matching. *Proceedings of the AAAI Conference on Artificial Intelligence* 36, 7 (Jun. 2022), 7594–7602. <https://doi.org/10.1609/aaai.v36i7.20725>
- [43] Andreas Loukas. 2020. How hard is to distinguish graphs with graph neural networks? *Advances in neural information processing systems* 33 (2020), 3465–3476.
- [44] Linyuan Lü and Tao Zhou. 2011. Link prediction in complex networks: A survey. *Physica A: statistical mechanics and its applications* 390, 6 (2011), 1150–1170.
- [45] Haggai Maron, Heli Ben-Hamu, Hadar Serviansky, and Yaron Lipman. 2019. Provably powerful graph networks. *Advances in neural information processing systems* 32 (2019).
- [46] Haggai Maron, Heli Ben-Hamu, Nadav Shamir, and Yaron Lipman. 2018. Invariant and Equivariant Graph Networks. In *International Conference on Learning Representations*.
- [47] Grégoire Mialon, Dexiong Chen, Margot Selosse, and Julien Mairal. 2021. Graphit: Encoding graph structure in transformers. *arXiv preprint arXiv:2106.05667* (2021).
- [48] Gaspard Michel, Giannis Nikolentzos, Johannes F Lutzeyer, and Michalis Vazirgiannis. 2023. Path neural networks: Expressive and accurate graph neural networks. In *International Conference on Machine Learning*. PMLR, 24737–24755.
- [49] Christopher Morris, Nils M Kriege, Franka Bause, Kristian Kersting, Petra Mutzel, and Marion Neumann. 2020. TUDataset: A collection of benchmark datasets for learning with graphs. *arXiv preprint arXiv:2007.08663* (2020).
- [50] Christopher Morris, Gaurav Rattan, and Petra Mutzel. 2020. Weisfeiler and Leman go sparse: Towards scalable higher-order graph embeddings. *Advances in Neural Information Processing Systems* 33 (2020), 21824–21840.
- [51] Christopher Morris, Martin Ritzert, Matthias Fey, William L Hamilton, Jan Eric Lenssen, Gaurav Rattan, and Martin Grohe. 2019. Weisfeiler and leman go neural: Higher-order graph neural networks. In *Proceedings of the AAAI conference on artificial intelligence*. 4602–4609.
- [52] Ryan Murphy, Balasubramaniam Srinivasan, Vinayak Rao, and Bruno Ribeiro. 2019. Relational pooling for graph representations. In *International Conference on Machine Learning*. PMLR, 4663–4673.
- [53] Giannis Nikolentzos, George Dasoulas, and Michalis Vazirgiannis. 2020. k-hop graph neural networks. *Neural Networks* 130 (2020), 195–205.
- [54] Pál András Papp, Karolis Martinkus, Lukas Faber, and Roger Wattenhofer. 2021. Dropgnn: random dropouts increase the expressiveness of graph neural networks. *Advances in Neural Information Processing Systems* 34 (2021), 21997–22009.
- [55] Pál András Papp and Roger Wattenhofer. 2022. A Theoretical Comparison of Graph Neural Network Extensions. *arXiv preprint arXiv:2201.12884* (2022).
- [56] Wonpyo Park, Woong-Gi Chang, Donggeon Lee, Juntae Kim, et al. 2022. GRPE: Relative Positional Encoding for Graph Transformer. In *ICLR2022 Machine Learning for Drug Discovery*.
- [57] Victor M Preciado and Ali Jadbabaie. 2010. From local measurements to network spectral properties: Beyond degree distributions. In *49th IEEE Conference on Decision and Control (CDC)*. IEEE, 2686–2691.
- [58] Chendi Qian, Gaurav Rattan, Floris Geerts, Mathias Niepert, and Christopher Morris. 2022. Ordered Subgraph Aggregation Networks. In *Advances in Neural Information Processing Systems*.
- [59] Raghunathan Ramakrishnan, Pavlo O Dral, Matthias Rupp, and O Anatole Von Lilienfeld. 2014. Quantum chemistry structures and properties of 134 kilo molecules. *Scientific data* 1, 1 (2014), 1–7.
- [60] Ladislav Rampáček, Michael Galkin, Vijay Prakash Dwivedi, Anh Tuan Luu, Guy Wolf, and Dominique Beaini. 2022. Recipe for a general, powerful, scalable graph transformer. *Advances in Neural Information Processing Systems* 35 (2022), 14501–14515.
- [61] Gaurav Rattan and Tim Seppelt. 2023. Weisfeiler-Leman and Graph Spectra. In *Proceedings of the 2023 Annual ACM-SIAM Symposium on Discrete Algorithms (SODA)*. SIAM, 2268–2285.
- [62] Dylan Sandfelder, Priyesh Vijayan, and William L Hamilton. 2021. Ego-gnns: Exploiting ego structures in graph neural networks. In *ICASSP 2021–2021 IEEE International Conference on Acoustics, Speech and Signal Processing (ICASSP)*. IEEE, 8523–8527.
- [63] Nino Shervashidze, SVN Vishwanathan, Tobias Petri, Kurt Mehlhorn, and Karsten Borgwardt. 2009. Efficient graphlet kernels for large graph comparison. In *Artificial intelligence and statistics*. PMLR, 488–495.
- [64] Behrooz Tahmasebi, Derek Lim, and Stefanie Jegelka. 2020. Counting substructures with higher-order graph neural networks: Possibility and impossibility results. *arXiv preprint arXiv:2012.03174* (2020).
- [65] Petar Veličković, Rex Ying, Matilde Padovano, Raia Hadsell, and Charles Blundell. 2019. Neural execution of graph algorithms. *arXiv preprint arXiv:1910.10593* (2019).
- [66] Clement Vignac, Andreas Loukas, and Pascal Frossard. 2020. Building powerful and equivariant graph neural networks with structural message-passing. *Advances in Neural Information Processing Systems* 33 (2020), 14143–14155.
- [67] Haorui Wang, Haoteng Yin, Muhun Zhang, and Pan Li. 2022. Equivariant and Stable Positional Encoding for More Powerful Graph Neural Networks. In *The Tenth International Conference on Learning Representations, ICLR 2022, Virtual Event, April 25–29, 2022*. OpenReview.net. <https://openreview.net/forum?id=e95i1IHcWj>
- [68] Zhili Wang, Shimin Di, and Lei Chen. 2023. A Message Passing Neural Network Space for Better Capturing Data-dependent Receptive Fields. In *Proceedings of the 29th ACM SIGKDD Conference on Knowledge Discovery and Data Mining (, Long Beach, CA, USA.) (KDD '23)*. Association for Computing Machinery, New York, NY, USA, 2489–2501. <https://doi.org/10.1145/3580305.3599243>
- [69] Boris Weisfeiler and Andrei Leman. 1968. The reduction of a graph to canonical form and the algebra which appears therein. *NTI, Series 2*, 9 (1968), 12–16.
- [70] Zonghan Wu, Shirui Pan, Fengwen Chen, Guodong Long, Chengqi Zhang, and S Yu Philip. 2020. A comprehensive survey on graph neural networks. *IEEE transactions on neural networks and learning systems* 32, 1 (2020), 4–24.
- [71] Zhenqian Wu, Bharath Ramsundar, Evan N Feinberg, Joseph Gomes, Caleb Geniesse, Aneesh S Pappu, Karl Leswing, and Vijay Pande. 2018. MoleculeNet: a benchmark for molecular machine learning. *Chemical science* 9, 2 (2018), 513–530.
- [72] Louis-Pascal Xhonneux, Andreea-Ioana Deac, Petar Veličković, and Jian Tang. 2021. How to transfer algorithmic reasoning knowledge to learn new algorithms? *Advances in Neural Information Processing Systems* 34 (2021), 19500–19512.
- [73] Keyulu Xu, Weihua Hu, Jure Leskovec, and Stefanie Jegelka. 2018. How Powerful are Graph Neural Networks?. In *International Conference on Learning Representations*.
- [74] Zuoyu Yan, Tengfei Ma, Liangcai Gao, Zhi Tang, and Chao Chen. 2021. Link prediction with persistent homology: An interactive view. In *International Conference on Machine Learning*. PMLR, 11659–11669.
- [75] Zuoyu Yan, Tengfei Ma, Liangcai Gao, Zhi Tang, and Chao Chen. 2022. Cycle representation learning for inductive relation prediction. In *International Conference on Machine Learning*. PMLR, 24895–24910.
- [76] Zuoyu Yan, Tengfei Ma, Liangcai Gao, Zhi Tang, Chao Chen, and Yusu Wang. 2023. Cycle Invariant Positional Encoding for Graph Representation Learning. In *The Second Learning on Graphs Conference*.
- [77] Zuoyu Yan, Tengfei Ma, Liangcai Gao, Zhi Tang, Yusu Wang, and Chao Chen. 2022. Neural Approximation of Graph Topological Features. In *Advances in Neural Information Processing Systems*, Alice H. Oh, Alekh Agarwal, Danielle Belgrave, and Kyunghyun Cho (Eds.).
- [78] Kuo Yang, Zhengyang Zhou, Wei Sun, Pengkun Wang, Xu Wang, and Yang Wang. 2023. EXTRACT and REFINe: Finding a Support Subgraph Set for

- Graph Representation. In Proceedings of the 29th ACM SIGKDD Conference on Knowledge Discovery and Data Mining (, Long Beach, CA, USA.) (KDD '23). Association for Computing Machinery, New York, NY, USA, 2953–2964. <https://doi.org/10.1145/3580305.3599339>
- [79] Tianjun Yao, Yingxu Wang, Kun Zhang, and Shangsong Liang. 2023. Improving the Expressiveness of K-hop Message-Passing GNNs by Injecting Contextualized Substructure Information. In Proceedings of the 29th ACM SIGKDD Conference on Knowledge Discovery and Data Mining (, Long Beach, CA, USA.) (KDD '23). Association for Computing Machinery, New York, NY, USA, 3070–3081. <https://doi.org/10.1145/3580305.3599390>
- [80] Chengxuan Ying, Tianle Cai, Shengjie Luo, Shuxin Zheng, Guolin Ke, Di He, Yanming Shen, and Tie-Yan Liu. 2021. Do transformers really perform badly for graph representation? Advances in Neural Information Processing Systems 34 (2021), 28877–28888.
- [81] Jiaxuan You, Jonathan M Gomes-Selman, Rex Ying, and Jure Leskovec. 2021. Identity-aware graph neural networks. In Proceedings of the AAAI Conference on Artificial Intelligence, 10737–10745.
- [82] Xingtong Yu, Zemin Liu, Yuan Fang, and Xinming Zhang. 2023. Learning to Count Isomorphisms with Graph Neural Networks. arXiv preprint arXiv:2302.03266 (2023).
- [83] Bohang Zhang, Shengjie Luo, Liwei Wang, and Di He. 2023. Rethinking the Expressive Power of GNNs via Graph Biconnectivity. In The Eleventh International Conference on Learning Representations, ICLR 2023, Kigali, Rwanda, May 1-5, 2023. OpenReview.net. <https://openreview.net/pdf?id=r9hNv76KoT3>
- [84] Muhan Zhang and Yixin Chen. 2018. Link prediction based on graph neural networks. Advances in neural information processing systems 31 (2018).
- [85] Muhan Zhang and Pan Li. 2021. Nested graph neural networks. Advances in Neural Information Processing Systems 34 (2021), 15734–15747.
- [86] Muhan Zhang, Pan Li, Yinglong Xia, Kai Wang, and Long Jin. 2021. Labeling trick: A theory of using graph neural networks for multi-node representation learning. Advances in Neural Information Processing Systems 34 (2021), 9061–9073.
- [87] Lingxiao Zhao, Wei Jin, Leman Akoglu, and Neil Shah. 2022. From Stars to Subgraphs: Uplifting Any GNN with Local Structure Awareness. In International Conference on Learning Representations.
- [88] Jie Zhou, Ganqu Cui, Shengding Hu, Zhengyan Zhang, Cheng Yang, Zhiyuan Liu, Lifeng Wang, Changcheng Li, and Maosong Sun. 2020. Graph neural networks: A review of methods and applications. AI Open 1 (2020), 57–81.
- [89] Yixiao Zhou, Ruiqi Jia, Hongxiang Lin, Hefeng Quan, Yumeng Zhao, and Xiaoping Lyu. 2023. Improving Graph Matching with Positional Reconstruction Encoder-Decoder Network. In Thirty-seventh Conference on Neural Information Processing Systems. <https://openreview.net/forum?id=28RTu9MOT6>
- [90] Wenhao Zhu, Tianyu Wen, Guojie Song, Liang Wang, and Bo Zheng. 2023. On Structural Expressive Power of Graph Transformers. In Proceedings of the 29th ACM SIGKDD Conference on Knowledge Discovery and Data Mining (, Long Beach, CA, USA.) (KDD '23). Association for Computing Machinery, New York, NY, USA, 3628–3637. <https://doi.org/10.1145/3580305.3599451>

## A THE WEISFEILER-LEMAN ALGORITHM AND MESSAGE PASSING NEURAL NETWORK

**1-WL.** We first describe the classic Weisfeiler-Leman algorithm (1-WL). For a given graph  $G$ , 1-WL aims to compute the coloring for each node in  $V$ . It computes the node coloring for each node by aggregating the color information from its neighborhood iteratively. In the 0-th iteration, the color for node  $v \in V$  is  $c_v^0$ , denoting its initial isomorphic type<sup>5</sup>. For labeled graphs, the isomorphic type of a node is simply its node feature. For unlabeled graphs, we give the same 1 to all nodes. In the  $t$ -th iteration, the coloring for  $v$  is computed as

$$c_v^t = \text{HASH}(c_v^{t-1}, \{\{c_u^{t-1} : u \in N(v)\}\})$$

, where HASH is a bijective hashing function that maps the input to a specific color. The process ends when the colors for all nodes between two iterations are unchanged. If two graphs have different coloring histograms in the end (e.g., different numbers of nodes with the same color), then 1-WL detects them as non-isomorphic.

**$k$ -WL.** For each  $k \geq 2, k \in \mathbb{N}$ , the  $k$ -dimensional WL algorithm ( $k$ -WL) colors  $k$ -tuples instead of nodes. In the 0-th iteration, the isomorphic type of a  $k$ -tuple  $\vec{v}$  is given by the hashing of 1) the tuple of colors associated with the nodes of the  $\vec{v}$ , and 2) the adjacency matrix of the subgraph induced by  $\vec{v}$  ordered by the node ordering within  $\vec{v}$ . In the  $t$ -th iteration, its coloring is updated by:

$$c_{\vec{v}}^t = \text{HASH}(c_{\vec{v}}^{t-1}, c_{\vec{v},(1)}^t, \dots, c_{\vec{v},(k)}^t)$$

, where

$$c_{\vec{v},(i)}^t = \{\{c_{\vec{u}}^{t-1} | \vec{u} \in N_i(\vec{v})\}\}, i \in [k]$$

Here,  $N_i(\vec{v}) = \{(v_1, \dots, v_{i-1}, w, v_{i+1}, \dots, v_k) | w \in V\}$  is the  $i$ -th neighborhood of  $\vec{v}$ . Intuitively,  $N_i(\vec{v})$  is obtained by replacing the  $i$ -th component of  $\vec{v}$  by each node from  $V$ . Besides the updating function, other procedures of  $k$ -WL are analogous to 1-WL. In terms of distinguishing graphs, 2-WL is as powerful as 1-WL, and for  $k \geq 2$ ,  $(k+1)$ -WL is strictly more powerful than  $k$ -WL.

**MPNNs.** MPNNs are a class of GNNs that learns node representations by iteratively aggregating messages from neighboring nodes. Let  $h_v^t$  be the node representation for  $v \in V$  in the  $t$ -th iteration. It is usually initialized with the node's intrinsic attributes. In the  $(t+1)$ -th iteration, it is updated by

$$h_v^{t+1} = W_1^t(h_v^t, \sum_{u \in N(v)} W_2^t(h_u^t, h_v^t, e_{uv}))$$

where  $W_1^t$  and  $W_2^t$  are two learnable functions. MPNN's power in terms of distinguishing non-isomorphic graphs is upper bounded by 2-WL [Xu et al. 2018].

## B THE PROOF OF THEOREM 4.2

We begin by introducing the *graph isomorphism*. For a pair of graphs  $G_1 = (V_1, E_1)$  and  $G_2 = (V_2, E_2)$ , if there exists a bijective mapping  $f: V_1 \rightarrow V_2$ , so that for any edge  $(u_1, v_1) \in E_1$ , it satisfies that  $(f(u_1), f(v_1)) \in E_2$ , then  $G_1$  is isomorphic to  $G_2$ , otherwise they are not isomorphic. Up to now, there is no polynomial algorithm for solving the graph isomorphism problem. One popular method is to use the  $k$ -order Weisfeiler-Leman [Weisfeiler and Leman 1968] algorithm ( $k$ -WL). It is known that 1-WL is as powerful as 2-WL, and for  $k \geq 2$ ,  $(k+1)$ -WL is more powerful than  $k$ -WL.

We then prove that  $k$ -WL can't count all connected substructures with  $(k+1)$  nodes (specifically,  $(k+1)$ -cliques). We restate the result as follows:

**Theorem B.1.** *For any  $k \geq 2$ , there exists a pair of graphs  $G$  and  $H$ , such that  $G$  contains a  $(k+1)$ -clique as its subgraph while  $H$  does not, and that  $k$ -WL can't distinguish  $G$  from  $H$ .*

**PROOF.** The counter-example is inspired by the well-known Cai-Fürer-Immerman (CFI) graphs [Cai et al. 1992]. We define a sequence of graphs  $G_k^{(\ell)}$ ,  $\ell = 0, 1, \dots, k+1$  as following,

$$V_{G_k^{(\ell)}} = \left\{ u_{a, \vec{v}} \mid a \in [k+1], \vec{v} \in \{0, 1\}^k \text{ and } \begin{cases} \vec{v} \text{ contains an even number of 1's,} & \text{if } a = 1, 2, \dots, k - \ell + 1, \\ \vec{v} \text{ contains an odd number of 1's,} & \text{if } a = k - \ell + 2, \dots, k + 1. \end{cases} \right\} \quad (5)$$

Two nodes  $u_{a, \vec{v}}$  and  $u_{a', \vec{v}'}$  of  $G_k^{(\ell)}$  are connected iff there exists  $m \in [k]$  such that  $a' \bmod (k+1) = (a+m) \bmod (k+1)$  and  $v_m = v'_{k-m+1}$ . We have the following lemma.

**Lemma B.2.** (a) *For each  $\ell = 0, 1, \dots, k+1$ ,  $G_k^{(\ell)}$  is an undirected graph with  $(k+1)2^{k-1}$  nodes;*

(b) *The set of graphs  $G_k^{(\ell)}$  with an odd  $\ell$  are mutually isomorphic; similarly, the set of graphs  $G_k^{(\ell)}$  with an even  $\ell$  are mutually isomorphic.*

<sup>5</sup>The term "isomorphic type" is based on previous work [Morris et al. 2019], which gives each  $k$ -tuple of nodes an initial feature such that two  $k$ -tuples receive the same initial feature if and only if their induced subgraphs (indexed by node order in the  $k$ -tuple) are isomorphic.

It's easy to verify (a). To prove (b), it suffices to prove  $G_k^{(\ell)}$  is isomorphic to  $G_k^{(\ell+2)}$  for all  $\ell = 0, 1, \dots, k-1$ . We apply a renaming to the nodes of  $G_k^{(\ell)}$ : we flip the 1<sup>st</sup> bit of  $\vec{v}$  in every node named  $u_{k-\ell, \vec{v}}$ , and flip the  $k^{\text{th}}$  bit of  $\vec{v}$  in every node named  $u_{k-\ell+1, \vec{v}}$ . Since this is a mere renaming of nodes, the resulting graph is isomorphic to  $G_k^{(\ell)}$ . However, it's also easy to see that the resulting graph follows the construction of  $G_k^{(\ell+2)}$ . Therefore, we assert that  $G_k^{(\ell)}$  must be isomorphic to  $G_k^{(\ell+2)}$ .

Now, let's ask  $G = G_k^{(0)}$  and  $H = G_k^{(1)}$ . Obviously there is a  $(k+1)$ -clique in  $G$ : nodes  $u_{j,0k}, j = 1, 2, \dots, k+1$  are mutually adjacent by definition of  $G_k^{(0)}$ . On the contrary, we have

**Lemma B.3.** *There's no  $(k+1)$ -clique in  $H$ .*

The proof is given below. Assume there is a  $(k+1)$ -clique in  $H$ . Since there's no edge between nodes  $u_{a, \vec{v}}$  with an identical  $a$ , the  $(k+1)$ -clique must contain exactly one node from every node set  $\{u_{a, \vec{v}}\}$  for each fixed  $a \in [k+1]$ . We further assume that the  $(k+1)$  nodes are  $u_{a, b_{a1}b_{a2}\dots b_{ak}}, a = 1, 2, \dots, k+1$ . Using the condition for adjacency, we have

$$b_{2k} = b_{11}, \tag{6}$$

$$b_{3k} = b_{21}, b_{3(k-1)} = b_{12}, \tag{7}$$

$$b_{4k} = b_{31}, b_{4(k-1)} = b_{22}, b_{4(k-2)} = b_{13}, \tag{8}$$

.....

$$b_{(k+1)k} = b_{k1}, b_{(k+1)(k-1)} = b_{(k-1)2}, \dots, b_{(k+1)1} = b_{1k}. \tag{9}$$

Applying the above identities to the summation

$$\sum_{a=1}^{k+1} \sum_{j=1}^k b_{aj} = 2 \sum_{j=1}^k (b_{1j} + b_{2j} + \dots + b_{(k-j+1)j}), \tag{10}$$

we see that it should be even. However, by definition of  $G_k^{(1)}$ , there are an even number of 1's in  $b_{a1}b_{a2}\dots b_{ak}$  when  $a \in [k]$ , and an odd number of 1's when  $a = k+1$ . Therefore, the sum in (10) should be odd. This leads to a contradiction.

Finally, to prove the  $k$ -WL equivalence of  $G$  and  $H$ , we have

**Lemma B.4.**  *$k$ -WL can't distinguish  $G$  and  $H$ .*

By virtue of the equivalence between  $k$ -WL and pebble games [Grohe and Otto 2015], it suffices to prove that Player II will win the  $C_k$  bijective pebble game on  $G$  and  $H$ . We state the winning strategy for Player II as following. Since  $G$  and  $H$  are isomorphic with nodes  $\{u_{k+1,*}\}$  deleted, Player II can always choose an isomorphism  $f: G - \{u_{k+1,*}\} \rightarrow H - \{u_{k+1,*}\}$  to survive if Player I never places a pebble on nodes  $u_{k+1,*}$ . Furthermore, since  $k$  pebbles can occupy nodes with at most  $k$  different values of  $a$  (in  $u_{a, \vec{v}}$ ), there's always a set of pebbleless nodes  $\{u_{a_0, \vec{v}}\}$  with some  $a_0 \in [k+1]$ . Therefore, Player II only needs to do proper renaming on  $H$  between  $u_{k+1,*}$  and  $u_{a_0,*}$  as stated above. This makes every  $\vec{v}$  in  $u_{a_0, \vec{v}}$  have an odd number of 1's. Player II then chooses the isomorphism on  $G - \{u_{a_0,*}\}$  and  $H^{\text{renamed}} - \{u_{a_0,*}\}$ . This way, Player II never loses since there are not enough pebbles for Player I to make use of the oddity at the currently pebbleless set of nodes.  $\square$

*Remark B.5.* Notice that if we take  $k = 2$ , then  $G$  is two 3-cycles while  $H$  is a 6-cycle, which 2-WL cannot differentiate; if we take  $k = 3$ , then  $G$  is the  $4^*4$  Rook's graph while  $H$  is the Shrikhande graph, which 3-WL cannot differentiate. In these special cases, the above construction complies with our well-known examples.

## C THE PROOF OF THEOREM 4.4

We restate the theorem as follows:

**Theorem C.1.** *For any connected substructure with no more than  $k+m$  ( $m \geq 2, k > 0$ ) nodes, there exists a subgraph GNN rooted at  $k$ -tuples with backbone GNN as powerful as  $m$ -WL that can count it.*

**PROOF.** Based on Remark 4.3 in the main paper, there exists a type of connected  $k$ -tuple that satisfies the decomposition of the connected substructure. Then the substructure can be separated into 2 subgraphs: the nodes that belong to the  $k$ -tuple (we call them rooted nodes) and the nodes that do not belong to the  $k$ -tuple (we call them non-rooted nodes). Formally, for the given two substructures  $G_1 = (V_1, E_1)$  and  $G_2 = (V_2, E_2)$ , we define the subgraph that formed by the rooted nodes of  $G_1$  ( $G_2$ , resp.) as  $G_{1,r} = (V_{1,r}, E_{1,r})$  ( $G_{2,r} = (V_{2,r}, E_{2,r})$ , resp.). Similarly, define the subgraph that formed by the non-rooted nodes of  $G_1$  ( $G_2$ , resp.) as  $G_{1,n} = (V_{1,n}, E_{1,n})$  ( $G_{2,n} = (V_{2,n}, E_{2,n})$ , resp.). We can also define the subgraph formed between the rooted nodes and non-rooted nodes of  $G_1$  ( $G_2$ , resp.) as  $G_{1,c} = (V_{1,c}, E_{1,c})$  ( $G_{2,c} = (V_{2,c}, E_{2,c})$ , resp.). Then it is easy to find that for  $G_1$ ,  $V_1 = (V_{1,r} \cup V_{1,n})$ ,  $V_{1,c} \subseteq V_1$ ,  $E_1 = E_{1,r} \cup E_{1,n} \cup E_{1,c}$ . There is no intersection between  $V_{1,r}$  and  $V_{1,n}$ , and there is no intersection between  $E_{1,r}$ ,  $E_{1,c}$ , and  $E_{1,n}$ . The same holds for  $G_2$ .

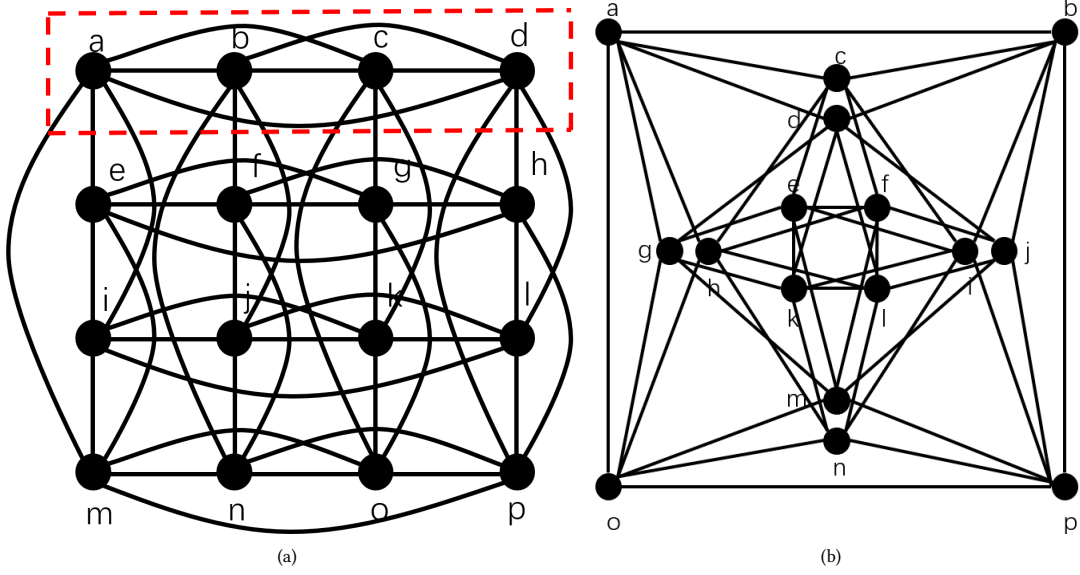


Figure 2: (a) the  $4 \times 4$  Rook Graph and (b) the Shrikhande Graph

If  $G_1$  and  $G_2$  are non-isomorphic, then there can be three potential situations: (1)  $G_{1,r}$  and  $G_{2,r}$  are non-isomorphic; (2)  $G_{1,n}$  and  $G_{2,n}$  are non-isomorphic; (3)  $G_{1,c}$  and  $G_{2,c}$  are non-isomorphic. In the following section, we will prove that in all these situations, the subgraph GNN can distinguish between  $G_1$  and  $G_2$ .

**$G_{1,r}$  and  $G_{2,r}$  are non-isomorphic.** It denotes that for  $G_1$  and  $G_2$ , the selected  $k$ -tuples are different. Then of course the subgraph GNN can differentiate  $G_1$  and  $G_2$ .

**$G_{1,n}$  and  $G_{2,n}$  are non-isomorphic.** Recall that we use a backbone GNN as powerful as  $m$ -WL to encode the information within the subgraph, and  $V_{1,n}$  and  $V_{2,n}$  contain nodes no more than  $m$  nodes. Therefore if  $G_{1,n}$  and  $G_{2,n}$  are non-isomorphic, then they will have different isomorphic types, and thus can be distinguished by the backbone GNN.

**$G_{1,c}$  and  $G_{2,c}$  are non-isomorphic.** We define the label of all nodes in  $G_1$  (the same holds for  $G_2$ ) as its distance to the nodes in the  $k$ -tuple. Formally, let  $V_{1,r} = \{v_{1,r,1}, \dots, v_{1,r,k}\}$ , then  $\forall u \in V_1$ , its label  $f_1(u) = (d(u, v_{1,r,1}), \dots, d(u, v_{1,r,k}), I(u))$ , where  $d(\cdot)$  denotes the shortest path distance between two nodes, and  $I(u)$  denotes the label that reflects the isomorphic type of  $u$  encoded by the subgraph GNN within  $G_{1,n}$ .

Since the substructures are connected, there exists at least a node  $u_1 \in V_{1,n}$ , whose label contains at least an index with the value "1". For  $f(u_1)$ , the indices with value "1" denotes that there exist edges between  $u_1$  and the corresponding nodes in  $V_{1,r}$ . While the indices with value larger than 1 denote that there is no edge between  $u_1$  and the corresponding nodes in  $V_{1,r}$ . The same holds for  $u_2$  and  $V_{2,r}$ . Therefore, if the subgraph formed by  $u_1$  and  $V_{1,r}$  and the subgraph formed by  $u_2$  and  $V_{2,r}$  are non-isomorphic, then  $f_1(u_1)$  and  $f_2(u_2)$  are different, and the subgraph GNN can differentiate the two substructures. Also, if the  $I(u_1)$  and  $I(u_2)$  are different, then the subgraph GNN can also distinguish  $G_1$  and  $G_2$ . We can then consider the next nodes, and continue the process inductively.

Therefore, if for all nodes in  $V_{1,n}$ , we can find a unique node in  $V_{2,n}$  that has the same label as it. Then  $G_{1,c}$  and  $G_{2,c}$  are isomorphic. Reversely, if  $G_{1,c}$  and  $G_{2,c}$  are non-isomorphic, then there exists at least a node in  $V_{1,n}$ , that we cannot find a unique node in  $V_{2,n}$  that has the same label as it. Therefore the subgraph GNN can differentiate  $G_1$  and  $G_2$ .

Then we can assign each substructure a unique color according to its isomorphic type, and use the color histogram of the graph as the output function. If two graphs have different numbers of certain substructures, then the color histogram will be different.

Based on the above results, the subgraph GNN can count the given type of connected substructure. □

## D THE PROOF OF THEOREM 5.4

We state the result as follows.

**Theorem D.1.** *ESC-GNN is strictly more powerful than 2-WL, while not less expressive than 3-WL.*

**PROOF. ESC-GNN is not less powerful than 3-WL.** As shown in Theorem 5.2, ESC-GNN is able to count 4-cliques. In the pair of graphs called the  $4 \times 4$  Rook Graph and the Shrikhande Graph (shown in Figure 2), there exist several 4-cliques in the  $4 \times 4$  Rook Graph, while there is no 4-clique in the Shrikhande Graph. Therefore ESC-GNN can differentiate the pair of graphs. Considering that 3-WL cannot differentiate them [Arvind et al. 2020], ESC-GNN is not less powerful than 3-WL.

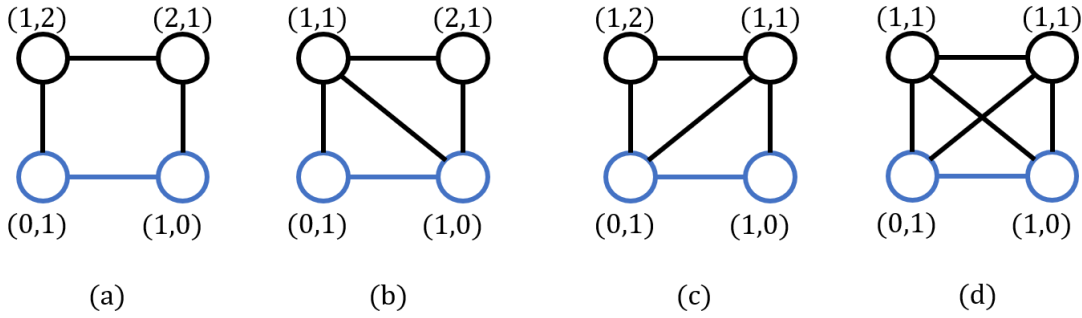


Figure 3: Examples of 4-cycles that pass the rooted edges. In these figures, the rooted 2-tuples are colored blue.

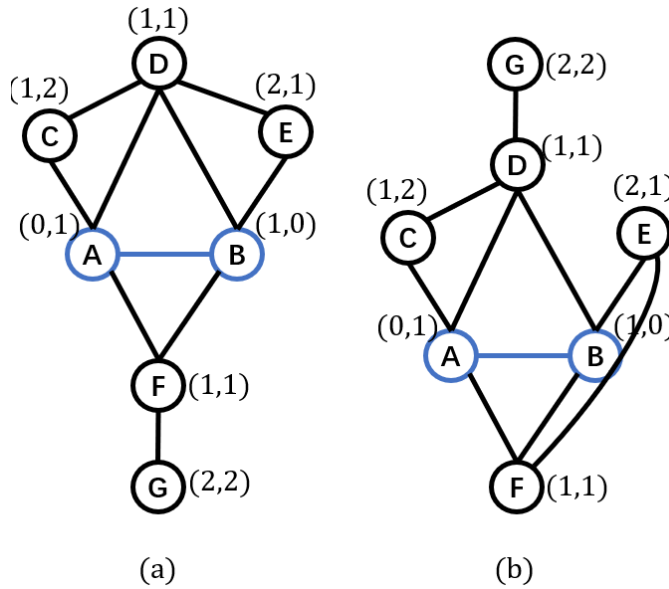


Figure 4: Examples where ESC-GNN cannot subgraph-count 5-cycles. In these figures, the rooted 2-tuples are colored blue.

**ESC-GNN is more powerful than 2-WL.** Using the MPNN [Xu et al. 2018] as the backbone network, it can be as powerful as 2-WL in terms of distinguishing non-isomorphic graphs. However, there exist pairs of graphs, e.g., the  $4 \times 4$  Rook Graph and the Shrikhande Graph that can be distinguished by ESC-GNN but not 2-WL. Therefore, ESC-GNN is strictly more powerful than the 2-WL. □

## E THE PROOF OF THEOREM 5.2

Below we show the counting power of ESC-GNN in terms of subgraph counting.

**Theorem E.1.** *In terms of subgraph counting, ESC-GNN can count (1) up to 4-cycles; (2) up to 4-cliques; (3) stars with arbitrary sizes; (4) up to 3-paths.*

**PROOF. Clique counting.** The number of 3-cliques is the number of nodes with the shortest path distance “1” to both rooted nodes; the number of 4-cliques is the number of edges labeled  $(1, 1, 1, 1)$  (definition see the edge-level distance encoding in Section 4 in the main paper, and example see Figure 3(d)). Therefore, ESC-GNN can count these types of cliques. In terms of 5-cliques, 4-WL cannot count them according to Theorem 4.2, therefore subgraph GNNs rooted on edges with MPNN as the backbone GNN cannot count 5-cliques according to Proposition 3.5 in the main paper. Then according to Proposition 4.1 in the main paper, ESC-GNN also cannot count 5-cliques.

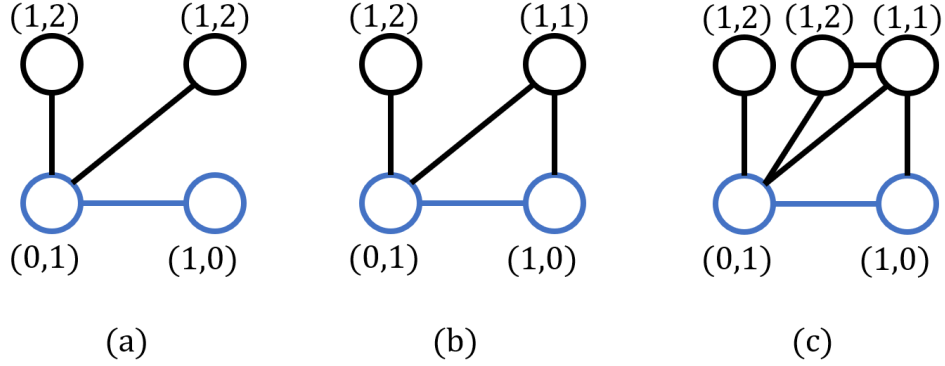


Figure 5: Examples of stars that pass the rooted edges. In these figures, the rooted 2-tuples are colored blue.

**Cycle counting.** the counting of 3-cycles is the same as 3-cliques. In terms of counting 4-cycles, there are basically 4 different situations where 4-cycles exist, examples are shown in Figure 3. Note that figures (a),(b), and (c) contain one 4-cycle, respectively, while figure (d) contains two 4-cycles that pass the rooted edge. Therefore the number of 4-cycles is the weighted sum of the number of edges with labels  $(1, 2, 2, 1)$ ,  $(1, 1, 2, 1)$ ,  $(1, 2, 1, 1)$ ,  $(1, 1, 1, 1)$ .

In terms of 5-cycle subgraph-counting, we provide a counter-example in Figure 4. In Figure 4(a), there is one 5-cycle  $ABEDC$  that passes  $AB$ , while there is no 5-cycle that passes  $AB$  in Figure 4(b). Considering that the degree information and the distance information is the same for the pair of graphs, ESC-GNN cannot differentiate them. Therefore, ESC-GNN cannot subgraph-count 5-cycles.

**Path Counting.** Note that the definition of paths here is different from other substructures. It denotes the number of edges within the path instead of the number of nodes within the path. Here, we slightly extend the use of 2-tuples in ESC-GNN by considering not only 2-tuples with edges but also 2-tuples without edges.

In terms of counting 2-paths or 3-paths between 2 nodes, it is equal to counting 3-cycles or 4-cycles, between edges, respectively. We have proven that ESC-GNN can count these cycles, therefore ESC-GNN can count such edges.

**Star counting.** We can decompose the graph-level star counting problem to 2-tuples by considering the first node of each 2-tuple as the root of stars. Examples are shown in Figure 5. We advocate that the number of stars is easily encoded by the number of nodes whose shortest path distance is 1 to the first rooted node. Denote the number of nodes with the shortest path distance 1 to the first rooted node as  $N'$  (including the second node), then the number of  $p$ -stars is  $C_{N'-1}^{p-2}$ . A similar proof is provided by [Chen et al. 2020].  $\square$

## F THE PROOF OF THEOREM 5.3

Below we show the counting power of ESC-GNN in terms of induced subgraph counting. We restate the Theorem 5.3 as follows.

**Theorem F.1.** *In terms of induced subgraph counting, ESC-GNN can count (1) up to 4-cycles; (2) up to 4-cliques; (3) up to 4-stars; (4) up to 3-paths.*

**PROOF. Clique counting.** Since cliques are fully connected substructures, the proof of cliques is the same as the proof of subgraph counting.

**Cycle counting.** For cycles, the number of 3-cycles is the same as 3-cliques. As for 4-cycles, we only need to consider the situation shown in Figure 3(a), where the number of  $(1, 2, 2, 1)$  edges reflects the number of 4-cycles. For induced-subgraph-counting 5-cycles, in Figure 7(a), there is no 5-cycle that pass  $AB$ , while in Figure 7(b), there is one 5-cycle  $ABEDC$  that passes  $AB$ . However, ESC-GNN cannot differentiate the two graphs since the degree information and the distance information is the same. Therefore, ESC-GNN cannot induced-subgraph-count 5-cycles. It can serve as the same example for not counting 4-paths.

**Path counting.** The proof of paths is actually the same as Theorem 5.2.

**Star counting.** In terms of 3-stars and 4-stars, we only need to consider the situation shown in Figure 5(a), where the number of  $(1, 2)$  nodes encodes the number of stars, i.e., denote the number of  $(1, 2)$  nodes as  $N'$ , the number of  $p$ -stars ( $p \leq 4$ ) is  $C_{N'}^{p-2}$ .

For 5-stars, a pair of examples are shown in Figure 6. These two graphs will be assigned the same structural embedding since the node degree information, and the distance information among these two graphs are the same. Therefore, ESC-GNN cannot differentiate the two graphs. However, Figure 6(a) contains no 5-star that passes the rooted 2-tuple  $AB$ , while Figure 6(b) contains one 5-star ( $BAFDG$ ) that passes the rooted 2-tuple  $AB$ .  $\square$



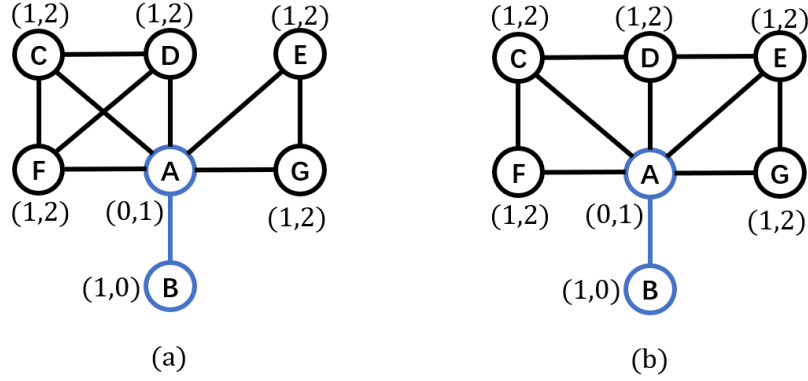


Figure 6: Examples where ESC-GNN cannot induced-subgraph-count 5-stars. In these figures, the rooted 2-tuples are colored blue.

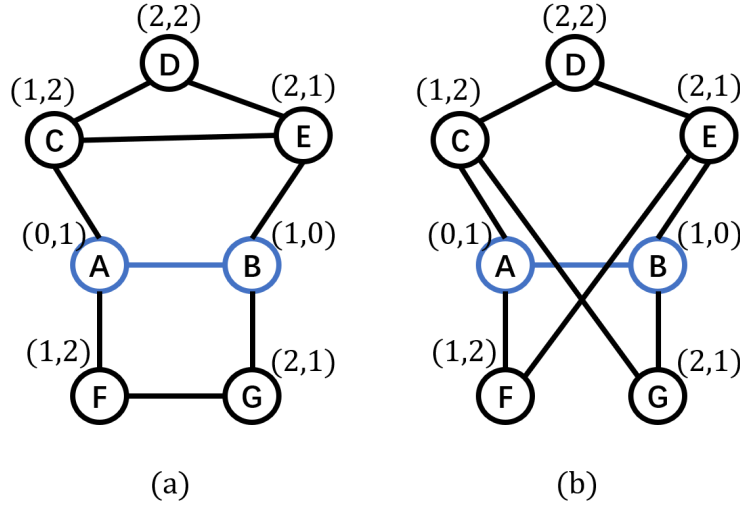


Figure 7: Examples where ESC-GNN cannot induced-subgraph-count 5-cycles. In these figures, the rooted 2-tuples are colored blue.

## G THE PROOF OF THEOREM 5.5

Here we restate Theorem 5.5 as follows:

**Theorem G.1.** Consider all pairs of  $r$ -regular graphs with  $n$  nodes, let  $3 \leq r < (2\log 2n)^{1/2}$  and  $\epsilon$  be a fixed constant. With the hop parameter  $h$  set to  $\lfloor (1/2 + \epsilon) \frac{\log 2n}{\log(r-1)} \rfloor$ , there exists an ESC-GNN that can distinguish  $1 - o(n^{-1/2})$  such pairs of graphs.

Recall that we encode the distance information as augmented structural features for ESC-GNN. For the input graph  $G$ , denote the node-level distance encoding on  $h$ -hop subgraphs on 2-tuple  $(u, v)$  as  $D_{(u,v),G}^{h,node}$ . Note that we can naturally transfer the encoding on 2-tuples to node by:  $(D_{v,G}^{h,node} = D_{(u,v),G}^{h,node})$ . We then introduce the following lemma.

**Lemma G.2.** For two graphs  $G_1 = (V_1, E_1)$  and  $G_2 = (V_2, E_2)$  that are randomly and independently sampled from  $r$ -regular graphs with  $n$  nodes ( $3 \leq r < (2\log 2n)^{1/2}$ ). Select two nodes  $v_1$  and  $v_2$  from  $G_1$  and  $G_2$  respectively. Let  $h = \lfloor (1/2 + \epsilon) \frac{\log 2n}{\log(r-1)} \rfloor$  where  $\epsilon$  is a fixed constant,  $D_{v_1,G_1}^{h,node} = D_{v_2,G_2}^{h,node}$  with probability at most  $o(n^{-3/2})$ .

**Table 7: Ablation study on the proposed structural embedding (norm MAE).**

Dataset	Tailed Triangle	Chordal Cycle	4-Clique	4-Path	Triangle-Rectangle	3-cycles	4-cycles	5-cycles	6-cycles
MPNN	0.3631	0.3114	0.1645	0.1592	0.2979	0.3515	0.2742	0.2088	0.1555
ESC-GNN	0.0052	0.0169	0.0064	0.0254	0.0178	0.0074	0.0044	0.0356	0.0337
(- MP)	0.062	1.9355	0.4124	0.0271	0.0563	0.1508	0.0050	0.0996	0.0443

**Table 8: The average number of substructures per graph/node in OGBG-HIV**

OGBG-HIV	3-cycle	4-cycle	5-cycle	6-cycle	tailed triangle	chordal cycle	4-clique	4-path	triangle-rectangle
graph	2.69e-2	3.69e-2	7.00e-1	2.28	1.02e-1	4.84e-3	2.43e-5	68.38	9.36e-3
node	3.16e-3	5.79e-3	1.37e-1	5.37e-1	4.01e-3	3.79e-4	7.63e-6	5.40	3.67e-4

**Table 9: The average number of substructures per graph/node in ZINC**

ZINC	3-cycle	4-cycle	5-cycle	6-cycle	tailed triangle	chordal cycle	4-clique	4-path	triangle-rectangle
graph	6.41e-2	1.60e-2	8.52e-1	1.80	8.79e-2	0	0	55.15	0
node	8.30e-3	2.76e-3	1.84e-1	4.67e-1	3.80e-3	0	0	4.76	0

PROOF. The proof follows from [Bollobás 1982; Feng et al. 2022]. As  $D_{v,G}^{h,node}$  stores exactly the same information as the node configuration used in [Feng et al. 2022], therefore the proof is exactly the same as the proof of Lemma 1 in [Feng et al. 2022].

Based on Lemma G.2, we can prove Theorem 5.5. Given node  $v_1 \in V_1$ , compare  $D_{v_1,G_1}^{h,node}$  with each  $D_{v_2,G_2}^{h,node}$  where  $v_2 \in V_2$ . The probability that  $D_{v_1,G_1}^{h,node} \neq D_{v_2,G_2}^{h,node}$  for all possible  $v_2 \in V_2$  is  $1 - o(n^{-3/2}) * n = 1 - o(n^{-1/2})$ . Therefore, ESC-GNN can distinguish  $1 - o(n^{-1/2})$  such pairs of graphs.  $\square$

## H DISCUSSION ON ESC-GNN’S EXPRESSIVE POWER THROUGH MESSAGE PASSING

In previous sections, we mainly discuss the expressive power enhanced by the proposed structural encoding. In this section, we shift to the integration of the global message passing layer and elucidate its substantial contribution to the expressive power. This is exemplified below through a toy example: consider graph  $G$ , composed of a 4-cycle and a 1-path (edge), and graph  $H$ , comprising a 5-path (a path with 6 nodes). When extracting 1-hop subgraphs for each node, both  $G$  and  $H$  yield two 1-paths and four "V graphs" (3 nodes and 2 edges). Consequently, the subgraph representation fails to distinguish between these two graphs. However, the introduction of a global message passing layer enables differentiation due to the distinct connections among these subgraphs. This distinction is applicable to both subgraph GNNs and our framework. Rattan and Seppelt [2023] provides a more comprehensive analysis, which substantiates that the global message passing can enhance expressiveness regardless of the choice of the hop parameter.

Additionally, We conduct an ablation study on the substructure counting dataset by removing the global message passing layer from ESC-GNN. The resulting new model, denoted as "(-MP)", relies solely on aggregating the structural encoding to derive the final prediction. Given the absence of additional node attributes, the new model can be easily implemented as ESC-GNN with a single message passing layer that aggregates the edge-level structural embedding to obtain the node-level prediction. The result is presented in Table 7. As evident from the table, ESC-GNN consistently outperforms the new model across all benchmarks, demonstrating that the global message passing layer significantly boosts the representation power of ESC-GNN.

## I DISCUSSION ON SUBSTRUCTURE COUNTING AND REAL-WORLD REPRESENTATION POWER

In this section, we discuss whether ESC-GNN’s representation power only benefits from its substructure-counting ability or not.

**Importance of substructures.** We incorporate an ablation study to show the importance of substructures in real-world tasks. The substructures, similar to Table 1, include 3-6 cycles, tailed triangles, chordal cycles, 4-cliques, 4-paths, and triangle-rectangles. We first report the number of these substructures at graph-level and node-level. Specifically, we report the average number of these substructures per graph (denoted as "graph") and the average number of these substructures that pass each node (denoted as "node"). The statistics are shown in Table 8 and Table 9.

Note that 6-cycles are commonly observed within these two graphs. On average, a graph contains approximately two 6-cycles, and there is an average incidence of 0.5 6-cycles that pass a node. This observation underscores the significance of 6-cycle, whose presence may potentially be attributed to the existence of benzene rings.

**Table 10: Analysis on the importance of substructures on real-world benchmarks**

Dataset	Baseline	3-cycle	4-cycle	5-cycle	6-cycle	tailed triangle	chordal cycle	4-clique	4-path	triangle-rectangle	all
ZINC	0.149	0.145	0.150	0.143	0.115	0.146	0.152	0.149	0.167	0.149	0.100
OGBG-HIV	73.89	73.48	74.67	74.47	73.60	73.69	71.98	73.56	68.40	53.18	71.47

**Table 11: Statistics of the used datasets.**

Dataset	Graphs	Avg Nodes	Avg Edges	Task Type	Metric
ZINC-12k	12000	23.2	24.9	Graph Regression	MAE
ZINC-250k	249456	23.1	24.9	Graph Regression	MAE
OGBG-HIV	41127	25.5	27.5	Graph Classification	AUC-ROC
QM9	129433	18.0	18.6	Graph Regression	MAE
Synthetic	5000	18.8	31.3	Node Regression	MAE

We then evaluate the significance of these substructures. In particular, we use a base GIN framework as the backbone network, and adopt the count of substructures that pass each node as the augmented node features. In Table 10, “all” denotes adding all these substructures as the augmented node feature. Due to the time limit, we only run the experiment twice and report the mean result.

**Analysis of the importance of substructures on real-world benchmarks.** We observe that in most cases, the number of substructures does not boost the performance either on ZINC or on OGBG-HIV. The only exception is that the number of 6-cycles boosts the performance on ZINC (maybe due to the information of benzene rings), and the number of all these substructures boosts the performance on ZINC. We present potential illustrations for the observation:

Firstly, in these molecule graphs, it is imperative to incorporate not only structural but also semantic information to enhance the model. For instance, it is well-established that molecular fingerprints can significantly elevate performance on the OGBG-HIV dataset (See [https://ogb.stanford.edu/docs/leader\\_graphprop/#ogbg-molhiv](https://ogb.stanford.edu/docs/leader_graphprop/#ogbg-molhiv)). In particular, the fingerprints contain the number of specific molecule structures, encompassing both the graph structures of molecules and the semantic information of atom types and bond types.

Secondly, the general distance information contains more structural information than the number of specific substructures, thus contributing more to real-world performance. For instance, we have proven that the number of 4-cycles can be computed using the distance information. Conversely, deducing distance information solely from the count of 4-cycles is impracticable, given the multiplicity of configurations that can form a 4-cycle.

## J EXPERIMENTAL DETAILS

**Statistics of Datasets.** The statistics of all used datasets are available in Table 11.

**Experimental details.** The baselines and data splittings of our experiments follow from existing works [Huang et al. 2023b; Zhang and Li 2021] and the standard data split setting. For ESC-GNN, we adopt GIN [Xu et al. 2018] as the backbone GNN (the only exception is that in Table 5, we use a plain graph transformer [Rampásek et al. 2022] as the backbone model for ZINC). In the structural embedding, we use both the shortest path distance and the resistance distance [Lü and Zhou 2011] as the distance feature. For the hop parameter  $h$  we search between 1 to 4, and report the best results. Following existing works [Huang et al. 2023b], we use Adam optimizer as the optimizer, and use plateau scheduler with patience 10 and decay factor 0.9. On most datasets, the learning rate is set to 0.001, and the hidden embedding dimension is set to 300. The training epoch is set to 2000 for counting substructures, 400 for QM9, 1000 for ZINC, and 150 for the OGB dataset. Most of the experiments are implemented with two Intel Core i9-7960X processors and 2 NVIDIA 3090 graphics cards. Others (e.g., experiments on the TU dataset) are implemented with two Intel Xeon Gold 5218 processors and 10 NVIDIA 2080TI graphics cards.

## K EVALUATION ON THE SPACE COST

With regards to the preprocessing time, our approach’s preprocessing time is comparable to that of  $I^2$ -GNN as shown in Table 3 in the main paper since we use their code to extract subgraph information. Although we require a small amount of extra time to extract and preprocess the structural embeddings, we believe that this is a reasonable trade-off since the actual model running time is reduced by orders. When compared to the total running time of subgraph GNNs, the preprocessing time is negligible. Therefore, our ESC-GNN’s total running time is less than 1% of that of  $I^2$ -GNN on ogbg-hiv.

As for the storage of structural embeddings, we only need to store a vector of integer indices for each structural embedding, as illustrated in Figure 1 in the main paper, without really storing any dense high-dimensional vectors. Therefore, the storage is still manageable. Specifically, when feeding the indices to the backbone model, we use a learnable matrix (which is a model parameter) to transform the integer index vector into dense embeddings. For example, to extract the degree information of the first subgraph in Figure 1 in the main paper, we use a

**Table 12: Evaluation on the space cost.**

Dataset	OGBG-HIV	ZINC	QM9
Original	159MB	16.2MB	281MB
NGNN	2.32GB	218MB	2.90GB
I <sup>2</sup> -GNN	5.95GB	627MB	8.25GB
ESC-GNN	2.57GB	427MB	4.46GB

learnable matrix  $W \in \mathbb{R}^{4 \times h}$  and compute the degree information with  $W * [0; 0; 4; 0]$ , where  $*$  denotes sparse matrix multiplication (which is very fast for sparse matrices), and the sparse vector  $[0; 0; 4; 0]$  is what we need to store. This approach requires relatively small storage space.

We have also included the space cost of our approach in Table 12. In these datasets, ESC-GNN requires much less storage space than I<sup>2</sup>-GNN while slightly more space than NGNN. These results demonstrate that our approach for storing structural embeddings offers excellent storage performance.

## L LIMITATIONS AND THE ASSETS WE USED

**Limitations of the paper.** First, we have shown that the representation power of our model is bounded by 4-WLs and subgraph GNNs rooted on 2-tuples in terms of distinguishing non-isomorphic graphs and counting substructures.

Second, the proposed model may not reach a satisfying performance on benchmarks where the encoded substructures are of no use. Also, the proposed model may not suit high-order graphs where the neighbors of the nodes and edges are defined differently from the simple graphs.

**The assets we used.** Our model is experimented on benchmarks from [Abboud et al. 2021; Balcilar et al. 2021; Dwivedi et al. 2020; Hu et al. 2020; Morris et al. 2020a; Murphy et al. 2019; Ramakrishnan et al. 2014; Wu et al. 2018; Zhao et al. 2022] under the MIT license.